

Open Loop and Closed Loop Cup Forming of Aluminum Sheet Metals

by

Pierre E. Jalkh

B.S., Mechanical Engineering
University of California at Davis, 1988

M.S., Mechanical Engineering
University of California at Davis, 1990

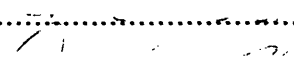
Submitted to the Department of Mechanical Engineering in Partial Fulfillment of the
Requirements for the

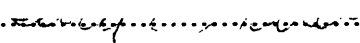
Mechanical Engineer's Degree

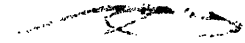
at the
Massachusetts Institute of Technology
January 1994

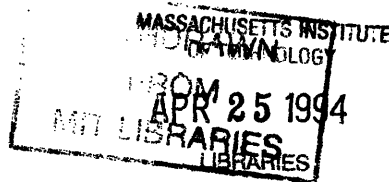
1994 Pierre E. Jalkh. All rights reserved.

The author hereby grants to MIT permission to reproduce and to distribute publicly paper
and electronic copies of this thesis document in whole or in part.

Signature of the Author.....


Certified by.....

David E. Hardt
Professor, Mechanical Engineering
Thesis Supervisor

Accepted by.....

Ain A. Sonin
Department of Mechanical Engineering
Chairman, Departmental Graduate Committee



**Open and Closed Loop Cup Forming
of Aluminum Sheet Metals
by**

Pierre E. Jalkh

submitted to the department of Mechanical Engineering on January 14, 1993
in partial fulfillment of the requirements for the Engineer's degree
in Mechanical Engineering

ABSTRACT

Most research in sheet metal forming have been concentrated on steel sheets. However, aluminum is an attractive candidate for forming research, since aluminum used for similar sheet metal products weighs 30% less than steel. Unfortunately, aluminum sheets do not form as deep as steel sheets. This thesis investigates the forming height of aluminum conical cups. The first part of the thesis involves constructing a forming height diagram for Al 2008-T4, Al 5754-HO and Al 6111-T4 for conical cup forming. Next, the forming height is shown to increase using a variable binder force trajectory. In the third part, the binder force is allowed to vary during the process by using a tangential force reference independent of process disturbances such as variation in the amount of lubrication and inadequate initial binder force. Finally, in order to improve the closed loop bandwidth, a tentative process model is presented.

Thesis supervisor: Dr. David E. Hardt

Title: Professor of Mechanical Engineering

Acknowledgments

First I would like to thank Professor David E. Hardt for his support, guidance, understanding and most importantly his patience throughout the duration of this research. I would also like to thank the research staff of Alcoa and Alcan for their financial support of the project and their technical assistance particularly Dr. James Story for his valuable suggestions.

I would also like to thank Professor Mary C. Boyce for her helpful advice and support and especially her enthusiasm. Special thanks also to Jian Cao for conducting simulations whenever I needed them without any complaint. Thank you Jian.

I would also like to thank members of the Sheet Metal Forming and Welding lab for their help and their friendship. Particularly, I would like to thank Jae Bok Song for his invaluable advice, and Dan Walczyk for both his advice and friendship. Also, my thanks go to Upendra Ummethala for his sincere friendship.

Thanks also to Fred Cote for all his help and also his friendship during the long hours in the machine shop. A special thanks also to the staff in the headquarters office, John Keene and Kathy Larson.

Finally, I would like to thank my parents, my sisters and brother for their love and support .

TITLE PAGE 1

ABSTRACT..... 2

ACKNOWLEDGMENTS..... 3

TABLE OF CONTENTS..... 4

CHAPTER 1 Introduction..... 6

 1.1 Motivation..... 6

 1.2 Preview of the Cup Forming Process..... 7

 1.3 Research Objective..... 8

CHAPTER 2 Issues in Aluminum Sheet Forming..... 12

 2.1 Introduction..... 12

 2.2 Immediate Advantages in Using Aluminum..... 12

 2.3 Disadvantages in Using Aluminum..... 12

 2.3.1 Quality..... 13

 2.3.2 Cost..... 14

CHAPTER 3 Experimental Procedure..... 16

 3.1 Introduction..... 16

 3.2 Experimental Procedure..... 16

 3.2.1 Conical Cup Experiments..... 16

 3.2.2 Lubrication..... 16

 3.2.3 Experiments..... 18

 3.2.4 Buckling and Fracture Limits for the Conical Cup 19

CHAPTER 4 Experimental Apparatus..... 20

 4.1 Introduction..... 20

 4.2 Physical Systems Connection..... 20

 4.3 The Punch Servosystem..... 22

 4.4 The Binder Servosystem..... 23

 4.5 The Buckle Detector..... 25

4.6 Flange Draw-in Measurement.....	26
CHAPTER 5 Results.....	28
5.1 Introduction.....	28
5.2 Open Loop Constant Binder Force Experiments.....	28
5.2.1 Results.....	28
5.2.2 discussion.....	31
5.3 Variable Binder Force Experiments.....	34
5.3.1 Introduction.....	34
5.3.2 Results.....	35
5.3.2.1 Trial Step Binder Force.....	35
5.3.2.2 Variable Binder Force trajectory.....	36
5.4 Closed Loop Tangential Force Forming.....	38
5.4.1 Introduction.....	38
5.4.2 Results.....	40
5.4.3 Discussion.....	43
CHAPTER 6 Conclusion, Present Research and Suggestions for Future Research.....	45
6.1 Summary and Conclusion.....	45
6.2 Present On-Going Research: Cup Forming Process Model.....	46
6.2.1 Method of Approach.....	46
6.2.2 Steady State Behavior.....	47
6.2.3 Transient Behavior.....	48
6.2.4 Decreasing Binder Force Dynamics.....	50
6.2.5 Closed Loop Simulation Results.....	51
6.2.6 Discussion and Suggestions for Future Research	52
Bibliography.....	56

Chapter 1

Introduction

1.1 Motivation

Lately there has been a growing interest to replace steel used in products by aluminum in the automotive industry. The immediate results are lighter, rust free products. The advantage in having lighter sheet metal products in automobiles is a lighter body and consequently a lighter frame which would result in saving material as well as in cutting down on gasoline consumption. The advantage in good rust protection properties is a longer lasting body which would not deteriorate under harsh environmental conditions.

In doing so, we encounter several issues that need to be explored before asserting whether Aluminum is an adequate replacement to Steel. Some of these issues are:

- **Hardness:** Steel possesses a higher hardness than Aluminum. It is true that Aluminum strain-hardens when it is deformed plastically, nevertheless the parts in the sheet that do not stretch or stretch very little will still be soft i.e. easily dented.
- **Abrasion:** Because of the aluminum oxide on the surface, aluminum is an extremely abrasive material. One major drawback in using aluminum instead of steel is the extreme wear that aluminum causes to dies used in forming the sheets. Die manufacturing is extremely expensive, therefore, before using aluminum one should study the cost incurred from increased Die wear.
- **Cost of Aluminum sheets:** Increased die wear is not the only cost to be taken into account; one should add the increased cost from using Aluminum sheets which are more expensive than steel sheets.
- **Springback:** Aluminum is known to have a larger springback than steel. By that we mean that a formed sheet of steel has a higher tendency to retain its shape than an aluminum sheet. In order to control the shape variation in aluminum sheets due to springback, one has to carefully control the strain paths during the forming process. This can be achieved by actively adjusting the clamping (or binder) force in order to follow the desired strain paths. In Cup Forming, this method became known as the Active Binder Force Control (see references [8] and [9]).
- **Formability:** Steel has better forming properties than aluminum. In other words, given two sheets, one of steel and the other of aluminum, steel will form to a much greater depth. In order to form aluminum to depths comparable to those of steel, we need to use

aluminum sheets twice as thick. Although the previous issues will be addressed, the issue of formability will be the focus of this research. One of the most commonly used processes to judge the formability of a material is the Cup Forming process.

1.2 Preview of the Cup Forming Process

Conical Cup Forming is a good way to test the formability of a given material. The geometry used is designed to mimic a stamping operation during the stage prior to the closure of the die sets. In a typical stamping operation, we can identify three sections of the material as shown in figure 1.1:

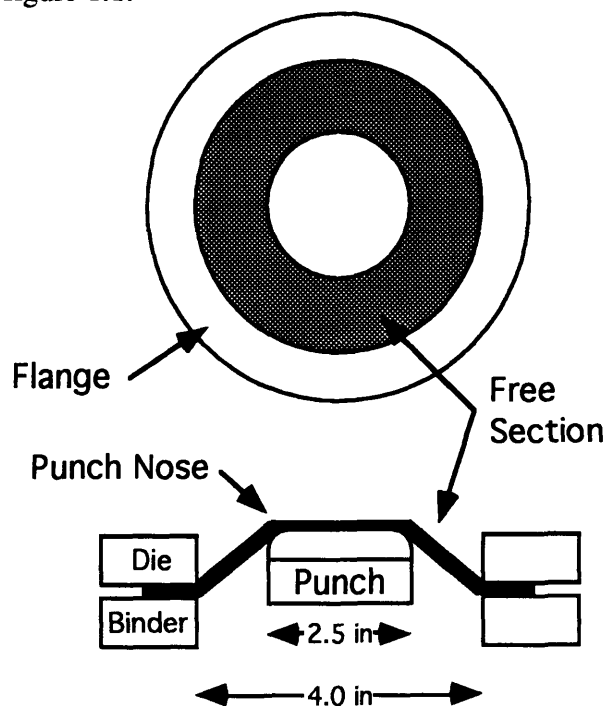


Figure 1.1 Schematic of the Cup Forming Process.

- The part under the punch or the set of dies that stretches very little during the forming process.
- The Flange: the part under the binder or the holding rings that draws in during the forming process.
- The Free Section: the part between the punch and the binder where the material is completely unsupported. This section is particularly susceptible to wrinkling during the process.

The conical geometry chosen in the Cup Forming process is designed to have the above three sections because they are characteristic of the sections in the stamping process.

1.3 Research Objective

This research is concerned with performing the standard open loop experiments on aluminum specimens in order to determine the maximum forming height and the corresponding clamping or binder force as shown in figure 1.2. The successful forming height is the height to which the cup can be formed without any wrinkling occurring in the free section or any tearing occurring near the punch nose.

Next, the goal is to devise a forming method to increase the forming height by altering the strain paths during the forming process. We achieve this by varying the binder force as shown in figure 1.3. Finally, the ultimate goal is to repeat the previous experiments using closed loop techniques in order to achieve the strain path desired and make the whole process robust to lubrication disturbances. During the open loop experiments, we record a history of the punch force in the part. Using geometry and a free body diagram we calculate the tangential force in the sheet shown in figure 1.4. This tangential force contains information about the tangential stresses near the punch nose where the part is most likely to fail due to tearing. We then replay this history (for the case where the binder force was optimum) as a reference signal in a closed loop scheme where we measure the punch force, calculate and feed back the actual tangential force in the part. See figure 1.5. In the case where the closed loop experiments do not track the desired forming conditions, the goal would then be to determine an open loop process model. This model would then be used to devise a control algorithm that would track the desired forming conditions.

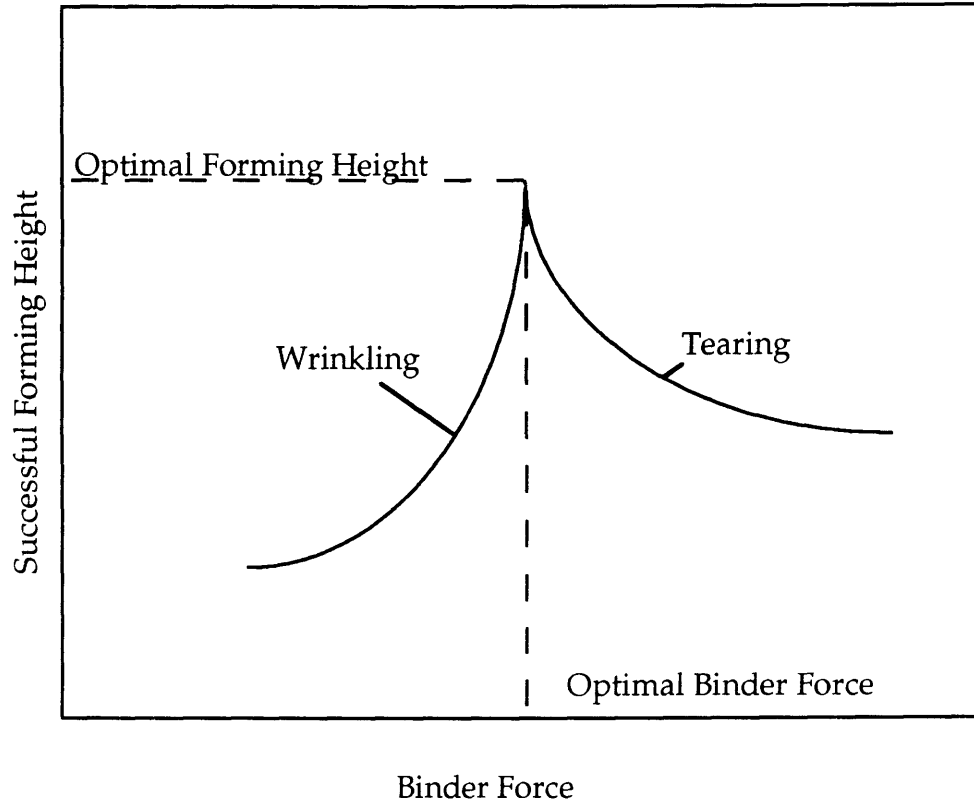


Figure 1.2. Typical Failure Height Curve for Constant Binder Force Forming Experiments.

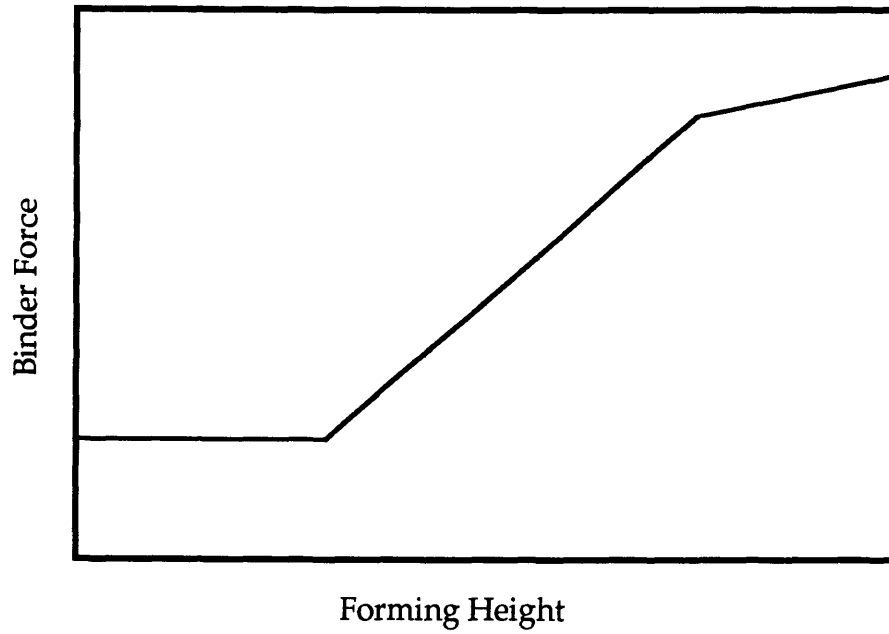


Figure 1.3 Variable Binder Force Trajectory. Improved Successful Forming Height.

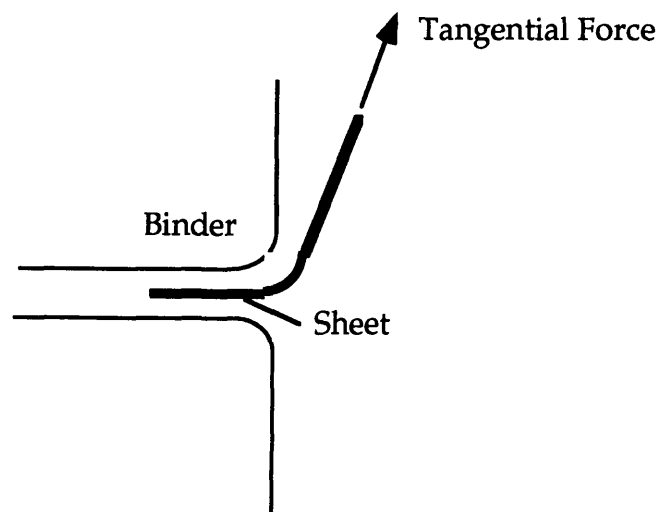


Figure 1.4 Diagram of the Tangential Force in the Sheet.

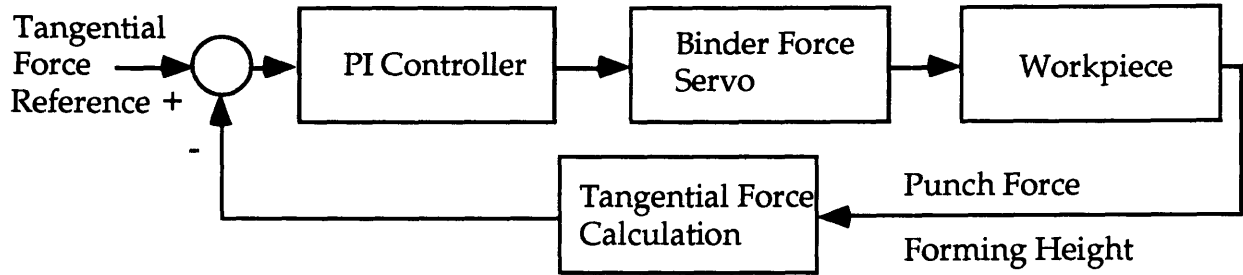


Figure 1.5 Tangential Force Control System Block Diagram.

1.4 Thesis Overview

The second chapter of this thesis presents the background information along with discussing all the issues in sheet metal forming mentioned above except the issue of formability.

The third chapter describes the experimental procedures as well as the method of approach used in the open loop constant binder force experiments, the closed loop tangential force feedback experiments and the open loop variable binder force experiments.

The fourth chapter briefly discusses the press used, and the measuring instruments. A brief discussion of the dynamics of the servosystems and their effects on the forming dynamics in case the process is speeded up. For further details of the press see Reference [8].

The fifth chapter presents the results obtained from open loop experiments of three aluminum alloys and a comparative study is presented. The variable binder force experiments and the closed loop results of tangential force references (obtained from open loop experiments) are also reported and discussed.

The sixth chapter discusses the open loop experiments. A comparative study between the aluminum alloys and previous steel experiments is presented and the reasons for the differences in forming results are mentioned. The closed loop experiments are discussed and the need for such experiments is stressed. Also, the problems encountered while doing these experiments are mentioned. These problems lead to the need for a process model. At this point, the process dynamics are extensively discussed and a tentative process model is presented.

This chapter also contains the conclusions from all these experiments and suggestions for future research.

Chapter 2

Issues in Aluminum Sheet Metal Forming

2.1 Introduction

Although the study undertaken involves examining and improving the forming process of aluminum alloy sheets, issues such as cost, weight, rust protection properties as well as the quality of the products obtained, should be addressed when assessing the use of a certain material. In this chapter, some of the advantages and the disadvantages of using aluminum instead of steel in sheet metal forming will be briefly discussed.

2.2 Immediate Advantages in Using Aluminum Alloys for Sheet Metal Forming

The use of aluminum sheets as a substitute for steel sheets results in lighter products. For example, in cup forming in order to form aluminum cups successfully to depths comparable to those of steel cups, one needs to use aluminum sheets twice as thick. The resulting steel to aluminum weight ratio is 1.44.

$$\frac{W_{steel}}{W_{alum}} = 1.44.$$

If the aluminum sheet were to replace a steel sheet in a car for example, the body would be 30% lighter. In addition, the frame of the car could also be lighter since it is supporting less weight.

In addition, aluminum alloys possess good rust protection properties which results in longer lasting products that do not deteriorate under harsh environmental conditions.

2.3 Disadvantages in Using Aluminum Alloys for Sheet Metal Forming

Although aluminum is a very attractive candidate for sheet metal forming, there are several problems associated with its use both during forming and after the forming process. These problems can be divided into two categories: one associated with the quality of the formed product and the other with the cost.

2.3.1 Quality

The two problems associated with quality are the low hardness of aluminum and the large springback that it exhibits after forming. Table 2.1 shows the values of the hardness for both steel and aluminum under the Knoop test [4].

H_{Alum}	29-43 [HK]
H_{steel}	150 [HK]

Table 2.1

Clearly, steel possesses a hardness which is 3 to 4 times larger than aluminum alloys. If it is used in commercial products, aluminum sheets can be easily indented which is not desired. However, aluminum strain hardens when it is deformed plastically. Therefore, the indentation problem can arise only in products which possess sections that do not deform plastically or sections that deform very little under the stamping process. In the case of the cup forming process for example, while the original sheets could easily be indented, all of the cups formed possessed a high hardness and consequently could not be indented.

The other problem is associated with shape retention. Metal parts are known to recover elastically after bending.

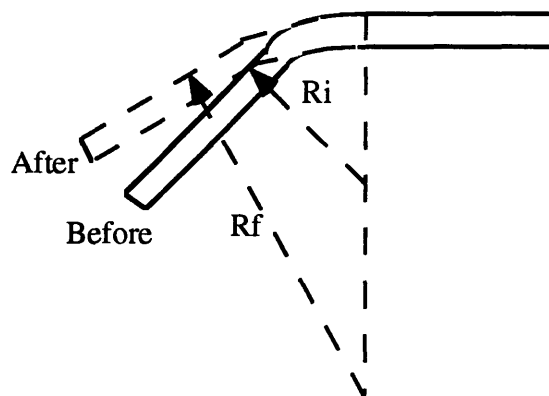


Figure 2.1 Springback in Bending.

Figure 2.1 shows a part that underwent some bending. The part was bent to an initial radius R_i , but the elastic part recovers to a new radius R_f . The springback formula is (reference [4]):

$$\frac{R_i}{R_f} = 4\left(\frac{R_i Y}{E T}\right)^3 - 3\left(\frac{R_i Y}{E T}\right) + 1 \quad (2.1)$$

where

R_i and R_f are the initial and final radii of curvature, Y , E and T are respectively the yield stress, the modulus of elasticity and the thickness of the material.

In most applications, since steel has a larger yield stress than aluminum, a steel part should retain its shape better than its aluminum counterpart. Nevertheless, in applications where the aluminum sheets need to have to be more than two times thicker than steel (for formability purposes), aluminum should exhibit about the same amount of springback as steel. In cup forming for example, the thickness of aluminum sheets used was twice as thick as steel sheets. Therefore, if an aluminum sheet and a steel sheet were bent over an initial radius of curvature

$$R_i = 1'' \quad (2.2)$$

then

$$\left(\frac{R_i}{R_f}\right)_{Al} = 0.715 \quad (2.3)$$

while

$$\left(\frac{R_i}{R_f}\right)_{steel} = 0.749 \quad (2.4)$$

Therefore, one should not expect aluminum sheets to springback anymore than steel sheets.

2.3.2 Cost

One of the major drawbacks from using aluminum is the high cost associated with it. First of all, sheets made out of aluminum used for an equivalent task as steel sheets cost about six times more. The cost ratio is between 6:1 and 7:1.

In addition, there is an increased cost associated with increased die wear due to the abrasive nature of aluminum oxide, the layer which usually covers aluminum sheets. The hardness of aluminum oxide is 2000-3000 HK. This hardness is about 13 to 20 times larger than the value of steel given in table 2.1.

Chapter 3

Experimental Procedure

3.1 Introduction

Conical Cup experiments are conducted to test the formability of a material. They are designed to mimic a typical stamping operation: Lubrication is used to enhance material draw-in under the binder while material is more restrained under the punch due to high contact forces with the tool. In the free area between the punch nose and the flange, the material is totally unsupported, unlike the Deep Drawing process where the wall and the punch support the material from both sides. In this area, the material is prone to wrinkling (since it is compressed in a smaller area) if the binder force is not sufficiently high. However if the binder force is too high, premature tearing occurs at the punch nose (where the radial stresses are highest). The basic test determines the relationship between the binder force and the maximum cup height at failure.

3.2 Experimental Procedure

3.2.1 Conical Cup Experiments

The punch and die used in these experiments are circular with the dimensions given below in Table 3.1. The radii of the punch and die as well as their radii of curvature are chosen in such a way as to simulate a real stamping operation as mentioned above. A smaller punch was used (2 “ diameter) but it allowed too much stretching on top. A bigger punch was not tried since the material would not draw in properly under such a condition. In summary, the geometries used were designed to allow decent flow of material in the unsupported region in order to get maximum forming height.

3.2.2 Lubrication

The lubrication used is a mixture of 3 parts 20W motor oil and 1 part STP oil (See reference [7]). The same amount of lubrication was used for all three materials (2.5cc on each side of the blank). The quantity was chosen to completely wet the area of the blank and to provide even lubrication throughout. Under these conditions the average friction coefficient under the binder is 0.1 while the coefficient under the punch is 0.3. These

results were obtained by conducting a compression torsion friction test where the frictional shear stress was measured under various levels of pressure for the material Al 2008-T4 and the lubricant mentioned above. For further details, see reference [14].

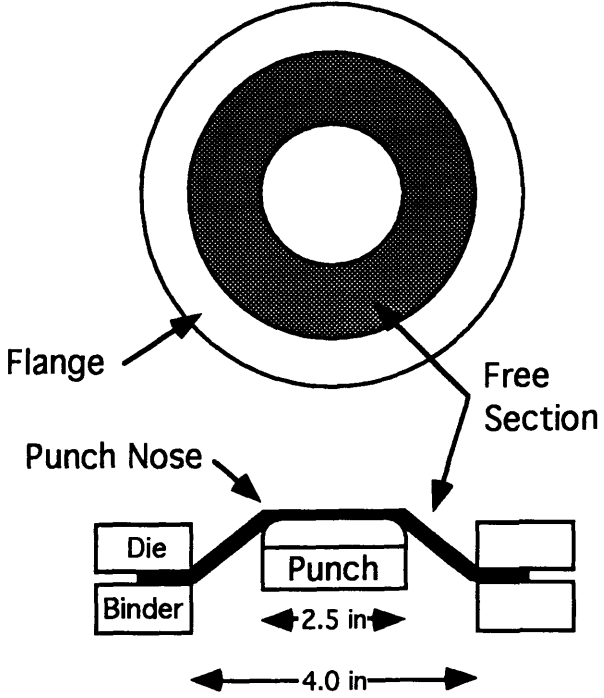


Figure 3.1 Schematic Of Cup Forming Process.

Blank Diameter [in]	6.250
Die Diameter [in]	4.020
Punch Diameter [in]	2.500
Die Profile Radius [in]	0.219
Punch Profile Radius [in]	0.250
Initial Binder Contact Area [sq. in]	17.99

Table 3.1

3.2.3 Experiments

All experiments for all materials were conducted at constant binder force. The punch speed is $0.015 \frac{\text{in}}{\text{sec}}$. The average strain rate used is $1.21 \times 10^{-3} \frac{\text{in}}{\text{in}\cdot\text{sec}}$. During the experiments, the binder force, punch force, punch position and flange draw-in were all monitored:

The binder force measurement is used in a force servo loop to ensure that the material is maintained at the desired clamping force throughout the experiment. The punch force provides information on the tangential stresses at the punch nose. Using the punch force data, we calculate the tangential force

$$F_t = \frac{F_p}{\sin\theta}$$

using geometry and a free body diagram as shown in figure 3.2.

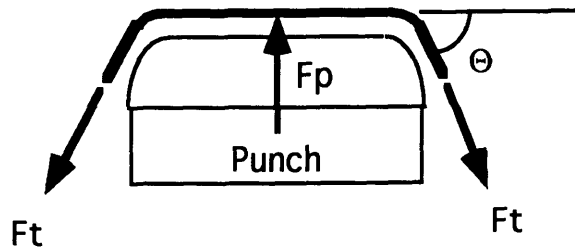


Figure 3.2 Free Body Diagram of the Section of the Sheet on Top of the Punch.

The punch position was measured using an LVDT which is calibrated periodically to maintain the position accuracy from one experiment to another.

The flange draw-in was measured using a lubricated string, anchored at one end, attached to an LVDT at the other, then wound once around the periphery of the sheet. In effect the measurement is an average of all the draw-in over the entire circumference of the blank. The draw-in is essential since it indicates how consistent the lubrication is between

two experiments at the same binder force as well as the difference in material flow between two experiments at different binder forces.

After the experiment, buckling in the unsupported area is also measured by turning the cup on a lathe and using a dial indicator which is directed normally to the surface of the unsupported area. Cups with wrinkles of amplitude above 0.002 in are declared failed.

3.2.4 Buckling And Fracture Limits For The Conical Cup

In all the experiments conducted, two modes of failure are identified:

i) Fracture at the top of the cup caused by sufficiently high binder forces.

ii) Buckling that usually starts in the flange and develops in the unsupported area because of insufficient binder force. Buckling which occurs in the unsupported region consists of high frequency variations in the radius of that region. In the case of all aluminum alloys, wrinkles also develop in the lower part of the unsupported region in the area near the flange.

Fracture is easily detected by a rapid drop in the punch force. The buckling limit cannot be detected from any single measurement and is instead determined by forming several cups at the same binder force but to different heights (0.025 inch apart). These cups are then examined, and the cups that have wrinkles of amplitude above 0.002 inch (lowest amplitude that is detectable by carefully feeling the cup with the fingers) were considered failed.

Chapter 4

Experimental Apparatus

4.1 Introduction

The apparatus used in the experiment was designed by Lee and Hardt. See Reference [8]. A picture of the press is shown in figure 4.1. It comprises a binder force servosystem, a punch position servosystem, and top and bottom plates separated by three columns. A detailed description of the design process and a description of the physical components can be found in Lee's Thesis. In this chapter, a brief description of the overall connection of the subsystems is presented and a discussion of the punch servosystem and the binder servosystem will follow. Most importantly, the dynamics of each of these subsystems will be discussed along with their effects on the process dynamics.

4.2 Physical Systems Connection

The press is completely computer controlled in the sense that every command given to any of the subsystems is initiated by the computer. Information on the performance of the subsystems is then returned to the computer which in turn adjusts to achieve adequate performance. Figure 4.2 shows a physical systems block diagram of each of the components and their interconnections along with the signal flow between them. The computer controls both the punch servosystem and the binder servosystem as shown in figure 4.2.

In the case of the punch servosystem, a voltage signal is sent through the I/O card to the system. The punch system itself is a position feedback system with a proportional controller. In this case, the position of the punch is also returned to the computer purely for measurement purposes.

In the case of the binder servosystem, the voltage signal is also sent through the I/O card to the binder system. The binder force is measured with a wheatstone bridge and returned to the computer which adjusts the signal (in the case where the feedback signal does not match the reference signal) using an integral controller. The binder system itself is a force feedback system with a proportional controller.

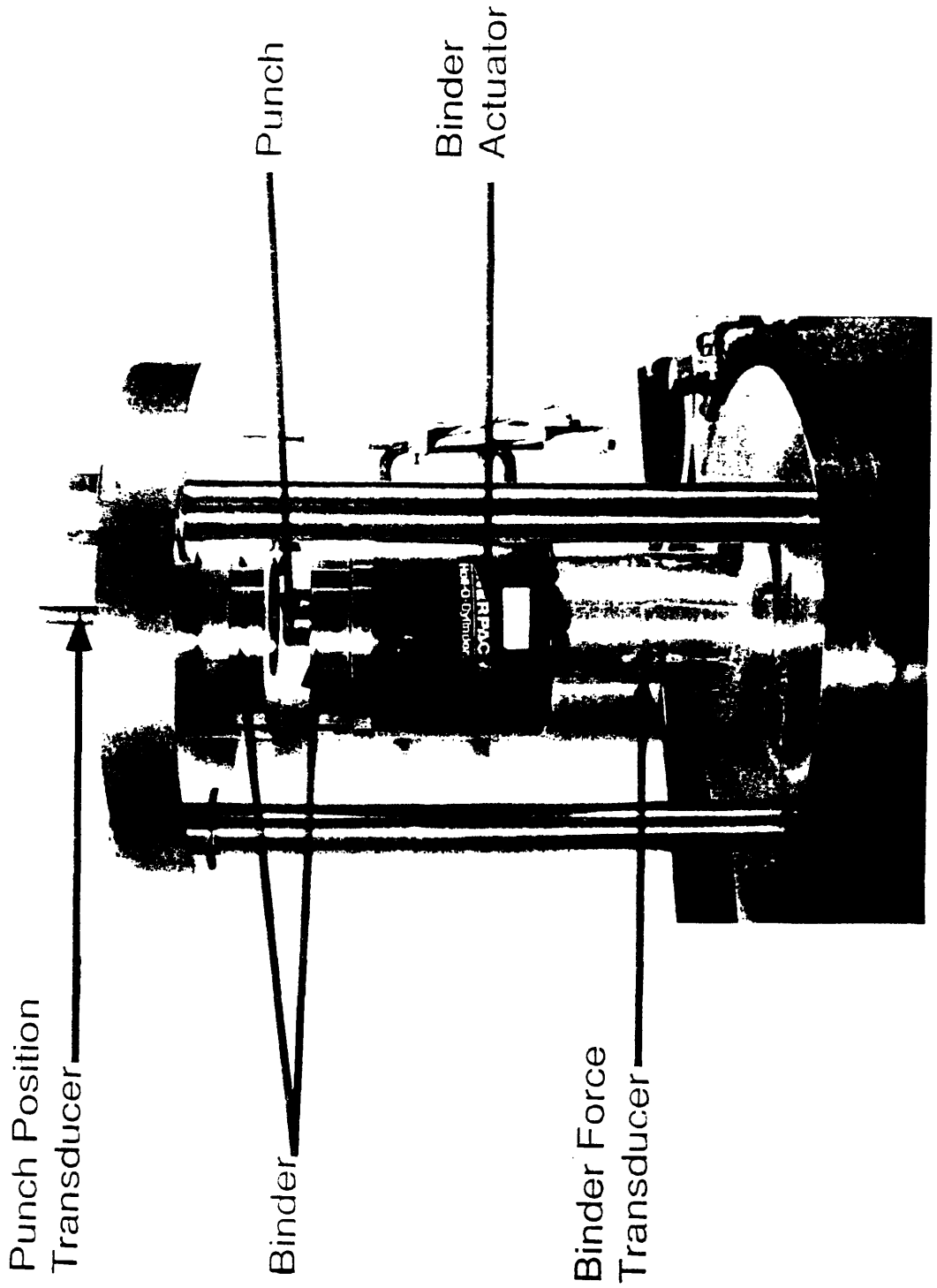


Figure 4.1 Photograph of The Press.

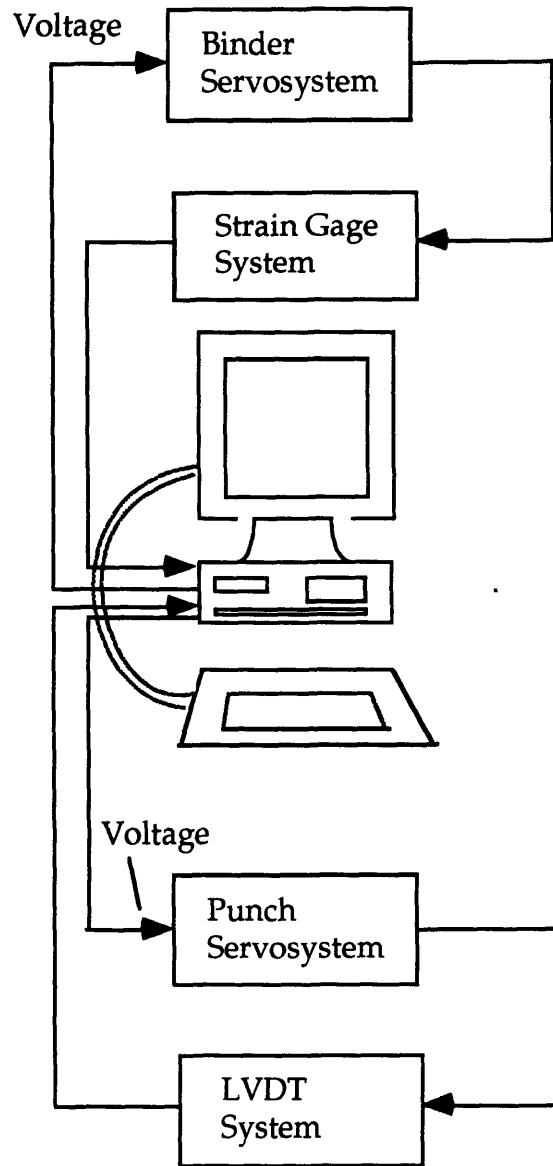


Figure 4.2 Physical Systems Block Diagram

4.3 The Punch Servosystem

The punch servosystem comprises several components some of which are mechanical while the others are electrical. A physical block diagram of the system is shown in figure 4.3. First the servocard: it sends a current to the high precision servovalve and receives the voltage from the LVDT which corresponds to the punch position. It compares

this voltage signal from the reference voltage signal received from the computer (shown in figure 4.2). Next the valve which is a flow control valve. It controls the fluid flow from the pump to the punch cylinder thereby controlling the pressure against the piston on which the punch rests. Finally, the punch position is read by the LVDT and returned to the servocard.

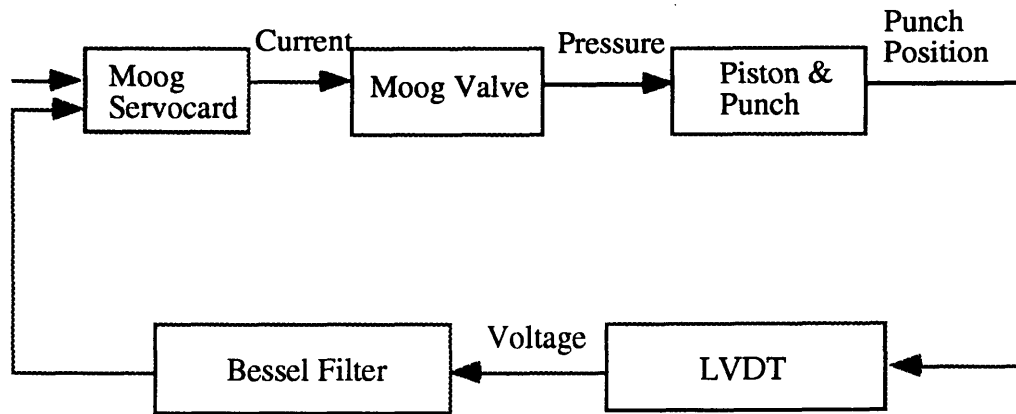


Figure 4.3 The Punch Servosystem.

4.4 The Binder System

In many ways, the binder system is similar to the punch system. Its block diagram is shown in figure 4.4. The voltage signal from the computer is sent to the servocard which drives the flow valve. The clamping force is measured using strain gages. The voltage signal from the bridge is filtered with a three pole Bessel filter of bandwidth 27 Hz. The filtered signal is then returned to the servocard where a proportional controller adjusts if a discrepancy exists between the reference voltage from the computer and the feedback signal from the bridge. The bandwidth of the binder servosystem was measured using an FFT signal analyzer. The cutoff frequency is 10 Hz. Since the binder feedback system still did not provide adequate performance of the binder, and a steady state error still existed between the reference signal and the output, an outer feedback loop with the computer as a digital integral controller has been added. Both the inner and the outer loop are shown in figure 4.5. As a result, the binder exhibits no steady state error with a bandwidth exceeding 5 Hz.

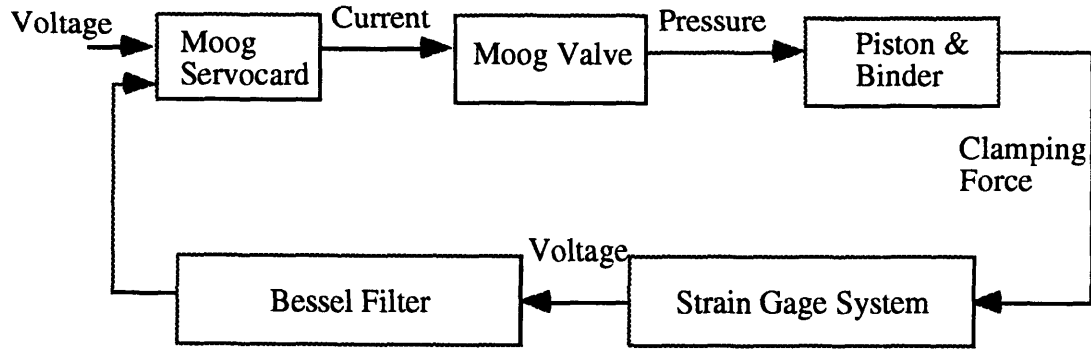


Figure 4.4 The Binder Servosystem

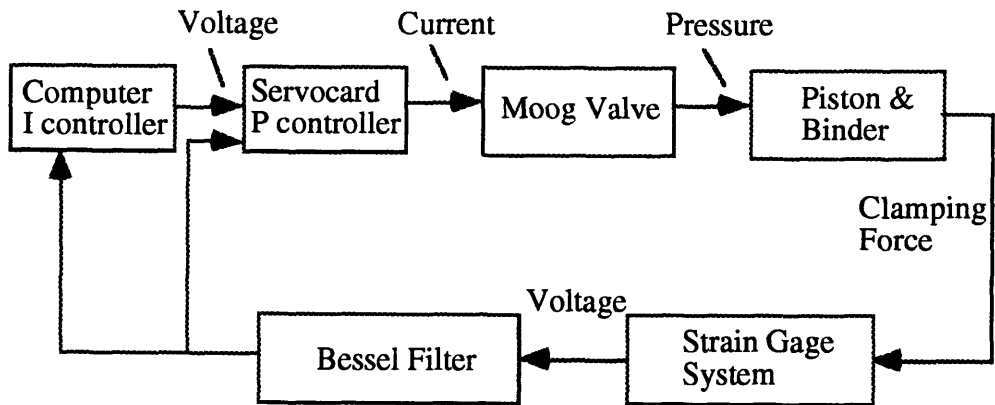


Figure 4.5 Inner and Outer Control Loop of the Binder System.

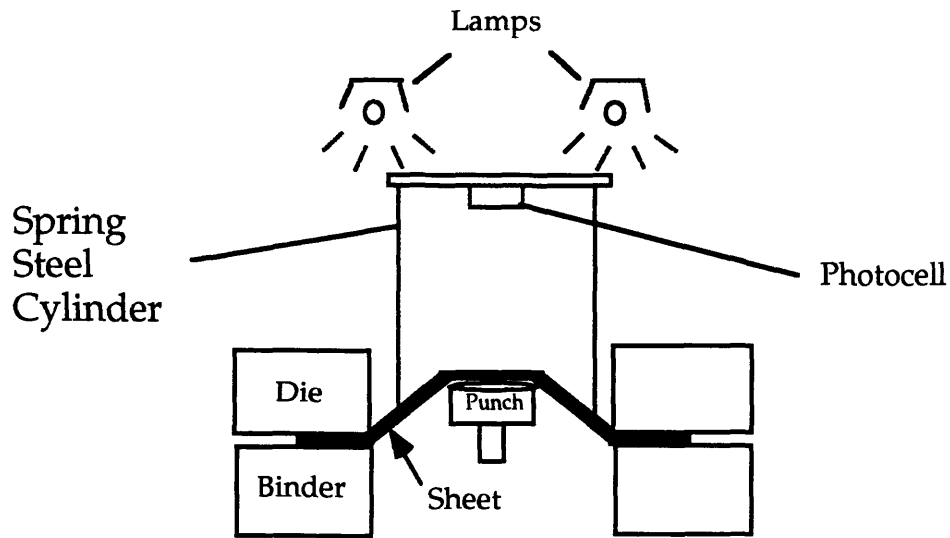


Figure 4.6 Schematic of the Buckle Detector.

4.5 The Buckle Detector

Failure due to buckling is not easy to detect. In the case of aluminum, small high frequency wrinkles can occur either in the upper portion of the unsupported region or in the flange then propagate to the lower portion of the unsupported region. To detect wrinkles occurring in the upper portion of the unsupported region, a simple device was constructed by Fenn [7]. Comprising a cylinder made of thin spring steel of a diameter that caused it to rest near the bottom of the unsupported region, the volume within the cylinder was sealed to light. The seal at the bottom was maintained provided that the cup remained round or slightly oval. When high frequency wrinkles appeared however, the seal was broken allowing light to enter the interior. By placing a resistive photocell in the interior, this light could be detected by noticing a gradual increase in the voltage signal across the photocell. In the case of steel sheets, this device proved to be very accurate. In the case of aluminum, however, wrinkles which developed in the lower portion of the unsupported region cannot be detected using this device. Fortunately, these wrinkles occurred at about the same stage as the wrinkles in the upper portion. So the buckle detector is only used as an initial approximation for detecting the onset of wrinkling. Further experiments had to be conducted by forming the cups to different heights (0.025 inch apart) and measuring the wrinkles by turning the cups on the lathe and using a dial indicator placed normal to the surface of the unsupported region. This measurement is shown in figure 4.7. This method is explained in details in the next chapter.

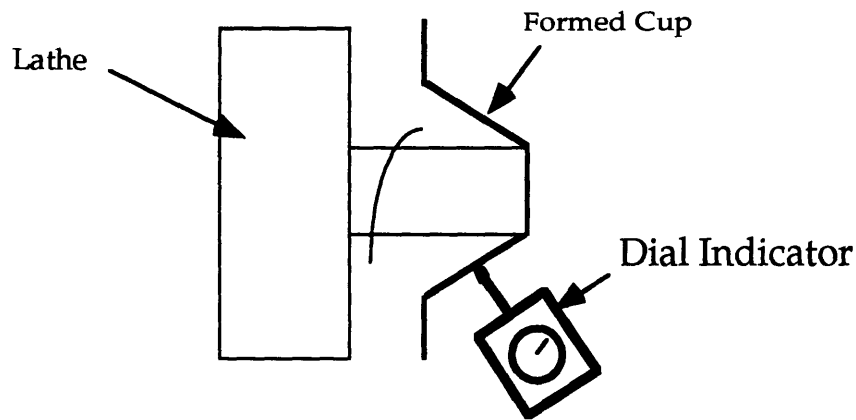
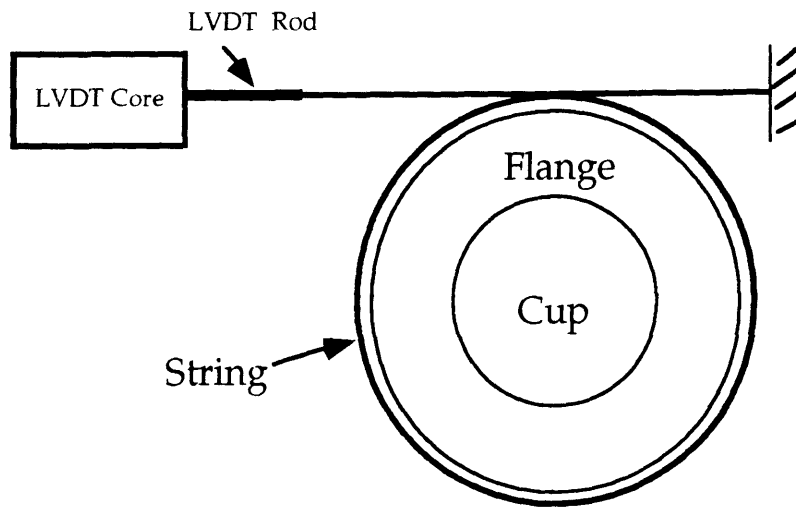


Figure 4.7 Buckling Measurement on the Lathe.

4.6 Flange Draw-in Measurement

The flange draw-in is essential since it indicates how consistent the lubrication is between two experiments at the same binder force as well as the difference in material flow between two experiments at different binder forces. The flange draw-in was measured using a lubricated string, anchored at one end, attached to an LVDT at the other, then wound once around the periphery of the sheet as shown in figure 4.8 (Top view). Another string, attached at the other end of the LVDT rod, is wound around a pulley where a weight is suspended from it keeping it taut (figure 4.8 side view). In effect, the measurement is an average of all the draw-in over the entire circumference of the blank.

Top View



Side View

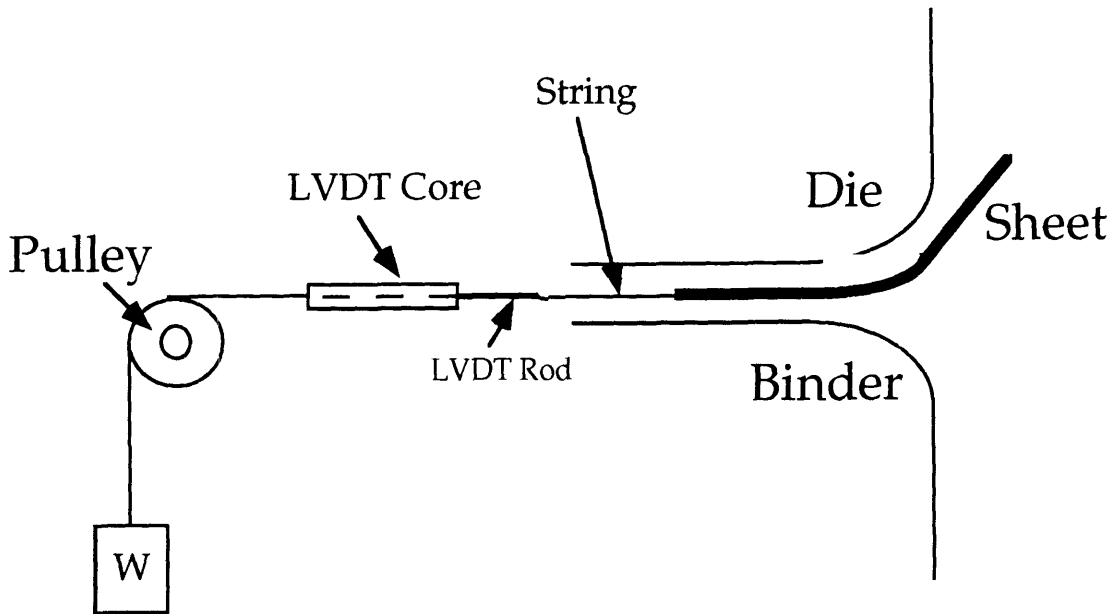


Figure 4.8 Schematic of the Draw-in Measurement System.

Chapter 5

Experimental Results

5.1 Introduction

The materials used are Al 2008-T4, Al 5754-HO and Al 6111-T4. As mentioned in chapter 3, the variables measured are the binder force (the input stage), the punch force (from which we calculate the tangential force) and the average draw-in. In this chapter, we present the results obtained from all the different experiments performed. The first set of experiments are the open loop constant binder force experiments. The second set of experiments consists of devising an open loop binder force trajectory which produces a better successful forming height. Finally, in the third set of experiments, we use the tangential force obtained from the experiment corresponding to optimal forming conditions as a reference input to a closed loop system where the binder force is at the input stage. This experiment is performed for different initial binder forces.

The open loop experiments are performed for two reasons:

- i) It allows us to find the optimal forming conditions (i.e. the optimal binder force)
- ii) It allows us to compare the formability of different materials and their sensitivity to binder force variations.

The variable binder force (or VBF) experiments are designed to improve the formability of a given material by varying the binder force during the process.

The closed loop experiments are designed to see if the results obtained by Fenn and Hardt [9] apply to aluminum alloys. The reasons for conducting these experiments are:

- i) By choosing the optimal tangential force trajectory as a reference for the closed loop forming system, we make the process independent of lubrication changes. Therefore if the amount of lubrication is not sufficient, the binder force will automatically compensate in order to submit the sheet to the optimal forming conditions.
- ii) By making the actual tangential force follow a prescribed trajectory, we are submitting all the parts to the same strain path. By doing so we obtain a better control over the shape variation between different parts due to springback.

5.2 Open Loop Constant Binder Force Experiments.

5.2.1 Results

These experiments were conducted by holding the binder force constant throughout the forming process. Several experiments were conducted some of which failed because of

tearing near the punch nose, while others failed because of wrinkling which occurred either in the unsupported area, or in the flange which later propagated to the unsupported area. In Figure 5.1, typical punch force data is shown for several binder forces. Figure 5.2 shows the tangential force responses, and figure 5.3 shows the average draw-in. In the case where the binder force was too high, tearing occurred prematurely and it can quickly be detected by a sudden drop in the punch force. If the binder force is not sufficiently high, wrinkling occurred. Its detection is very subtle, since one can only detect it after the fact by a slow leveling then a slow drop in the punch force. In order to determine the wrinkling limit several tests are conducted at the same binder force. Each of these tests was taken to different forming heights (0.025 inch apart). Wrinkling was then measured by turning the cup on a lathe with the aid of a dial indicator. Those cups with undulations of amplitudes above 0.002 inch were considered wrinkled. Figure 5.4 shows the forming height diagram for Al 5754-HO. The tearing limit is clear and consistent from one experiment to another. The wrinkling limit is more of a band since certain cups failed at a given height while others did not. All the experiments were repeated for the three aluminum alloys and the wrinkling limits as well as the tearing limits were determined. The forming height diagrams were drawn for all three alloys.

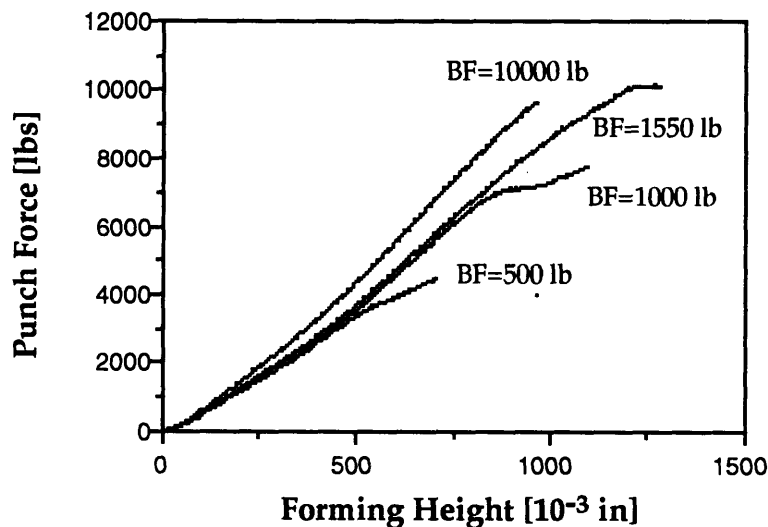


Figure 5.1 Punch Force Data For Binder Forces of 500, 1000, 1550 and 10000 lbs For Al 2008-T4.

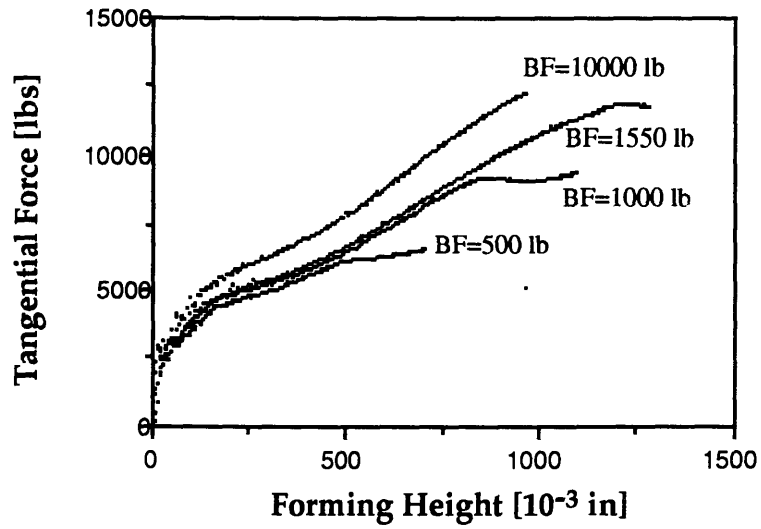


Figure 5.2 Tangential Force Data For Binder Forces of 500, 1000, 1550 and 10000 lbs For Al 2008-T4.

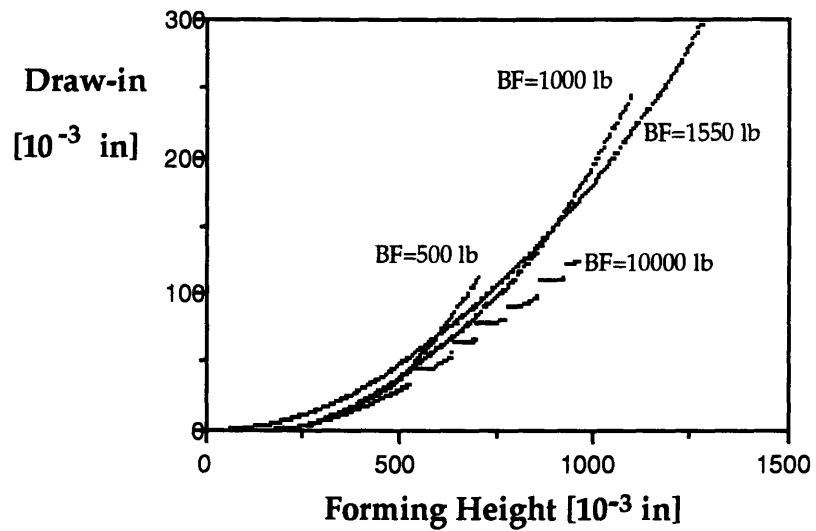


Figure 5.3 Draw-in Data For Binder Forces of 500, 1000, 1550 and 10000 lbs For Al 2008-T4.

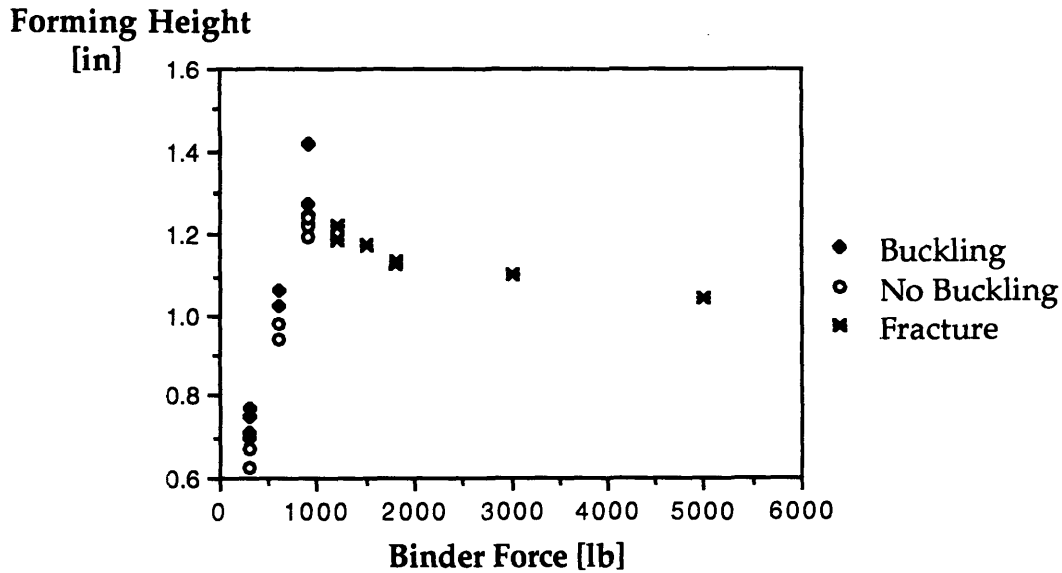


Figure 5.4 Forming Height Diagram For Aluminum Alloy 5754-H0.

5.2.2 Discussion

The results of the tests performed on all materials are shown in figure 5.5. Although all three materials seem to be equally formable¹, their corresponding optimal forming binder forces are quite different. The OBF (Optimal Binder Force) for Al 5754-H0 is at 900 lbf while the OBF for Al 2008-T4 and Al 6111-T4 is at 1500 lbf. Although the OBF's for all three materials are different, the draw-in at failure for optimum conditions was the same for all (within measurement errors) $.25 \pm .01$ inches.

In addition the flange wrinkling amplitude at failure is 0.055 inch for Al 2008-T4, 0.070 inch for 5754-H0 and 0.080 inch for 6111-T4. The fact that the high OBF's for the first and the last material did not affect flange wrinkling suggests that the binder force range involved in all tests is not high enough to suppress wrinkling in the flange due to high compressive hoop stresses. In particular, the experiments show that all three materials have comparable formability but the lubricant used provided lower apparent friction coefficient in the case of Al 2008-T4 and Al 6111-T4 than in the case of Al 5754-H0. From a practical perspective however, it did not provide any advantage since both draw-in and flange wrinkling are about the same for all materials at optimal conditions. All three aluminum alloys have very similar cup forming characteristics but the question remains how they compare with steel.

¹ Formable here means maximum possible height at failure.

Figure 5.6 shows the forming height diagrams for the aluminum alloys and AKDQ steel. Experiments on AKDQ steel were conducted by Fenn. (see Ref [8]). Sheets of 0.020 inch thickness (half the thickness of the aluminum alloys) were used. Obviously, the steel alloy has a better forming height at the optimum forming conditions. In addition, the optimum binder force for steel is much higher (6000 lbs). This suggests that the lubricant provided a much better friction coefficient for steel and therefore better controllability. In order to even consider using aluminum in place of steel in sheet metal forming, we need to devise a technique to improve the maximum forming height of aluminum.

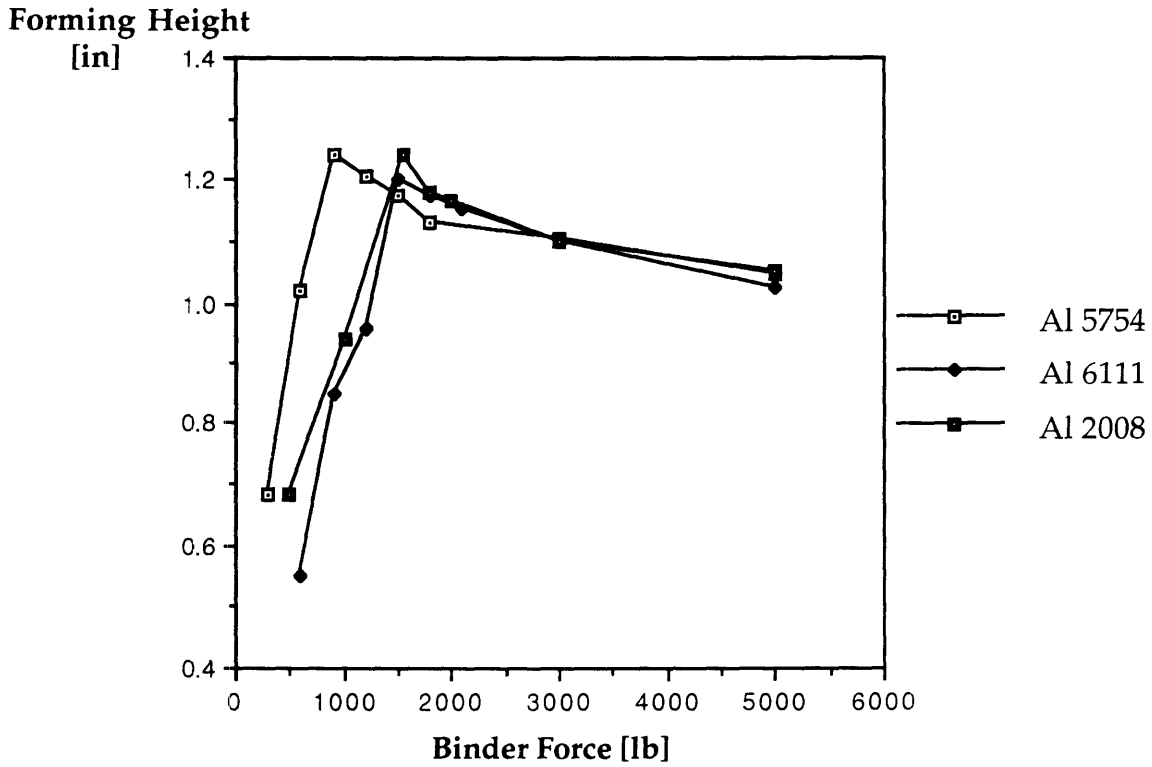


Figure 5.5 Forming Height Diagram For All Aluminum Alloys: 2008-T4, 5754-HO, 6111-T4.

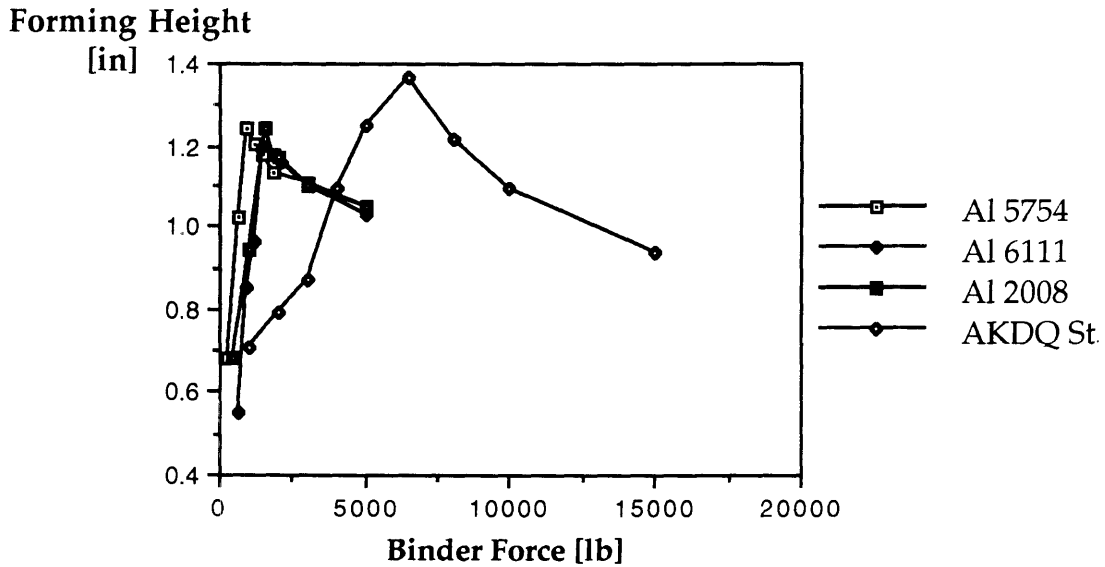


Figure 5.6 Forming Height Diagram for All Aluminum Alloys and AKDQ Steel.

5.3 Variable binder Force Experiments

5.3.1 Introduction

In this section we devise a binder force trajectory other than constant that will improve the maximum forming height. For this set of experiments, the alloy Al 2008-T4 was chosen since it possessed a slightly better forming height. In addition, its optimum binder force is the highest among the aluminum alloys which will provide us with more room to vary the binder force.

The work presented in this section has been preceded by other researchers. Hishida (see Ref [10]) suggested the trajectories shown in figure 5.7. All trajectories starting at high binder forces then decreasing did not succeed in suppressing the wrinkling. The trajectories that did succeed are the ones that start at low binder forces then increase during the process. The results obtained were successful but they were obtained by trial and error. In this section, we present a methodical approach in synthesizing the optimal binder force and we present the results obtained experimentally.

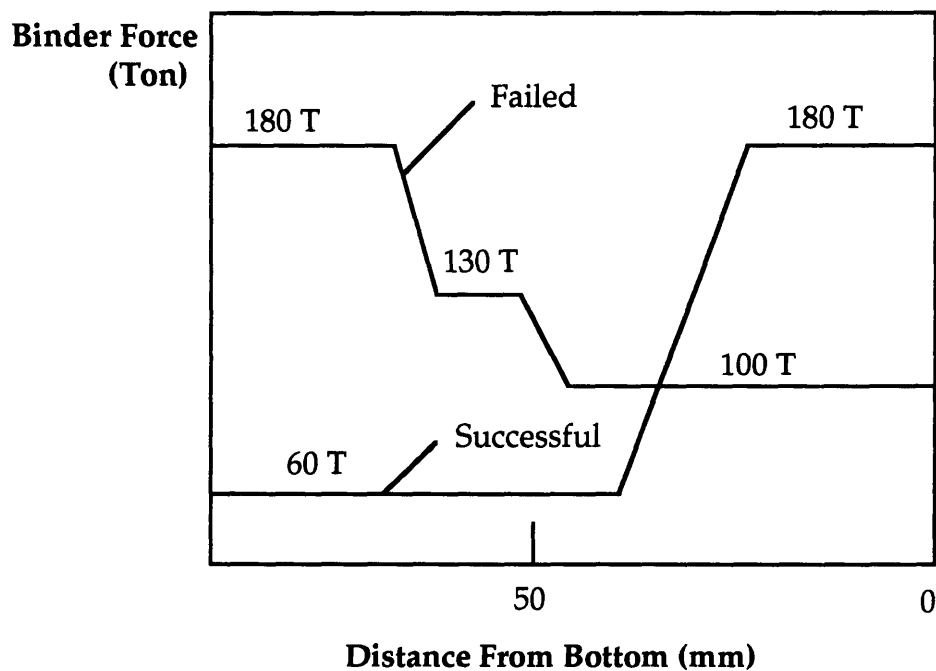


Figure 5.7 Binder Force Trajectory As Described By Hishida [10,11].

5.3.2 Results

5.3.2.1 Trial Step Binder Force Trajectory.

As mentioned earlier, the optimal constant binder force (or CBF) does not necessarily optimize the material flow for forming without any failure. After careful examination of the failure modes and the reason for their occurrence, improvement of the forming height may be found by varying the binder force during the process. Here, in order to make better use of the material in the flange, a low binder force of 500 lb is used. This method permits more material to draw into the unsupported area at the beginning of the process. The binder force is then stepped up to a force slightly greater than the optimal constant binder force (of 1500 lb) in order to prevent wrinkling from occurring. The idea behind this method is to stretch the material as little as possible early in the process. Therefore, during the critical and final stage, the material near the punch nose will be thick enough to withstand the high tangential stresses. The step increase was made at a forming height of 0.5 inch where severe wrinkling becomes apparent to the naked eye. Figure 5.9 shows a plot of the binder force trajectory used. Figure 5.10 shows a plot of the punch force corresponding to the constant binder force along with the punch force corresponding to the step binder force. Notice that the punch forces are very similar except for the kink in the latter. The forming results for the step binder force are not better but the type of failure mode is dramatically different. While the constant binder force experiment failed due to tearing near the punch nose, the step binder force experiment failed due to wrinkling in the unsupported area even though the final binder force was higher than the CBF. This supports our theory that if we let material move in the deformation zone early in the process, enough material thickness will be available in the latter stage to withstand the high tangential stresses. Therefore, by starting the process at low binder forces, we are able to delay the premature tearing near the punch nose. In addition, by increasing the binder force in the latter stage of the process, we are able to suppress the wrinkling in the unsupported area. Now the question becomes: Can we achieve the same results or perhaps improve the present results by varying the binder force in a continuous rather than the abrupt fashion ?

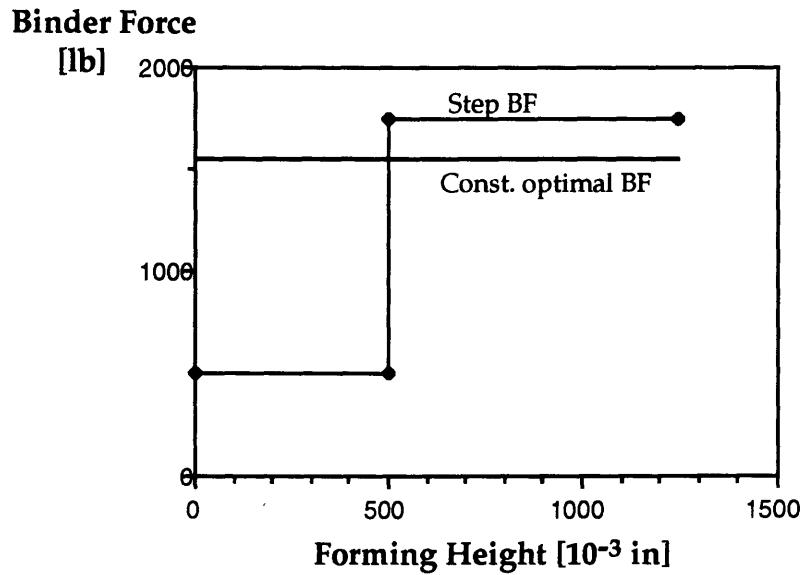


Figure 5.8 Optimal Constant Binder Force Trajectory and Step Trajectory.

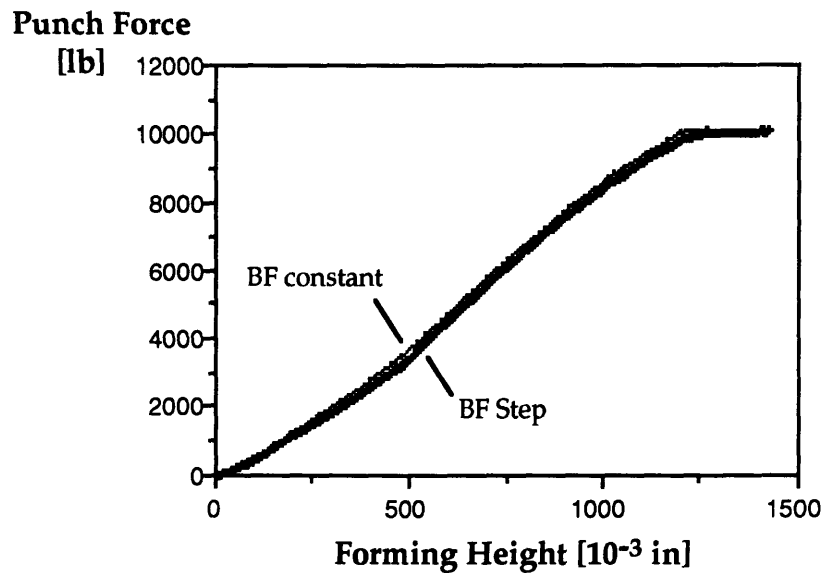


Figure 5.9 Punch Forces Corresponding to Constant Optimal Binder Force Trajectory and Step trajectory.

5.3.2.2 Variable Binder Force Trajectory (VBF).

As shown in the step binder force experiments failure by wrinkling or tearing can be delayed by varying the binder force during the forming process. The reason the problem

of improving the forming height is difficult to solve, lies in the fact that if we want to suppress wrinkling we increase the binder force therefore causing premature tearing in the part and vice-versa. The problem then becomes an optimization task: Increase the resistance of the material to tearing by keeping the binder force as low as possible while maintaining enough binder pressure to suppress the wrinkling in the flange. Therefore, the task is reduced to starting the process with a binder force close to zero. Whenever wrinkles appear in the flange, we increase the binder force to a new force that will suppress those wrinkles. We then maintain this new force until wrinkles reappear at which point we increase the binder force again. By iterating this procedure we obtain the staircase binder force shown in figure 5.10. Next, we smooth the staircase binder force trajectory by fitting two affine functions through it. The final stage of the process is to adjust the slopes of the affine functions in order to obtain the maximum successful failure height possible. We do by adjusting the slope of the first line first then the second line.

As a result of this iterative procedure, we obtain a new failure height of 1.385 inch. The new failure height is 11% higher than the optimal CBF failure height.

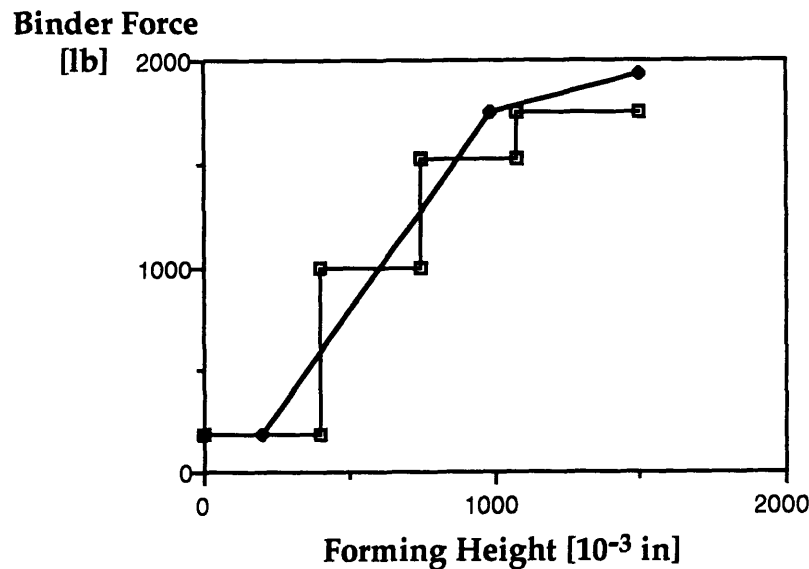


Figure 5.10 Multiple Step Binder Force Trajectory and Optimal Variable Trajectory.

As mentioned earlier, the problem of finding the maximum forming height for the process is an optimization problem. The task at hand is to form the cup by avoiding wrinkling and tearing at every stage of the process. This is exactly what is done when the VBF is used. Therefore, the binder force strategy adopted in figure 5.10 is optimal nevertheless it is hard to reproduce. As in the case of the CBF experiments, by slightly altering the amount of lubrication used, we can no longer obtain the new optimal forming height. In order to consistently obtain the maximum forming height one needs to devise a forming strategy which is independent of the lubrication conditions. In other words, by using the binder force as a reference to form the cups, the failure height may be compromised by the change in the friction conditions in the flange. In order to overcome this problem, the reference used for forming optimally should be a quantity which is independent of the amount of lubrication. Although the same goal can be achieved by using the binder force as a reference while carefully using the same amount of lubrication, in a typical stamping operation where time and statistical variations are costly one needs to devise a better scheme.

5.4 Closed Loop Tangential Force Forming

5.4.1 Introduction

The experiments and results discussed so far involve pre-determining a binder force be it constant or variable in order to obtain adequate forming conditions. As discussed above, a change in the lubrication conditions or even material surface finish could alter the optimum binder force trajectory. This problem is addressed here by constructing a closed loop process scheme that seeks to track a tangential force reference corresponding to the optimal binder force. See figure 5.11. This reference is obtained from the constant and variable binder force open loop experiments. Under this scheme, variations in friction conditions in the flange area will not shift the process away from the optimal conditions since the reference to be tracked is independent of these disturbances. The control system block diagram is used to actively control the binder force in real-time. The control algorithm used is a proportional integral controller. The gains used provide a stable response with moderate tracking speed for the tangential force corresponding to the CBF. Unfortunately, they do not provide a stable response for the VBF as will be discussed later.

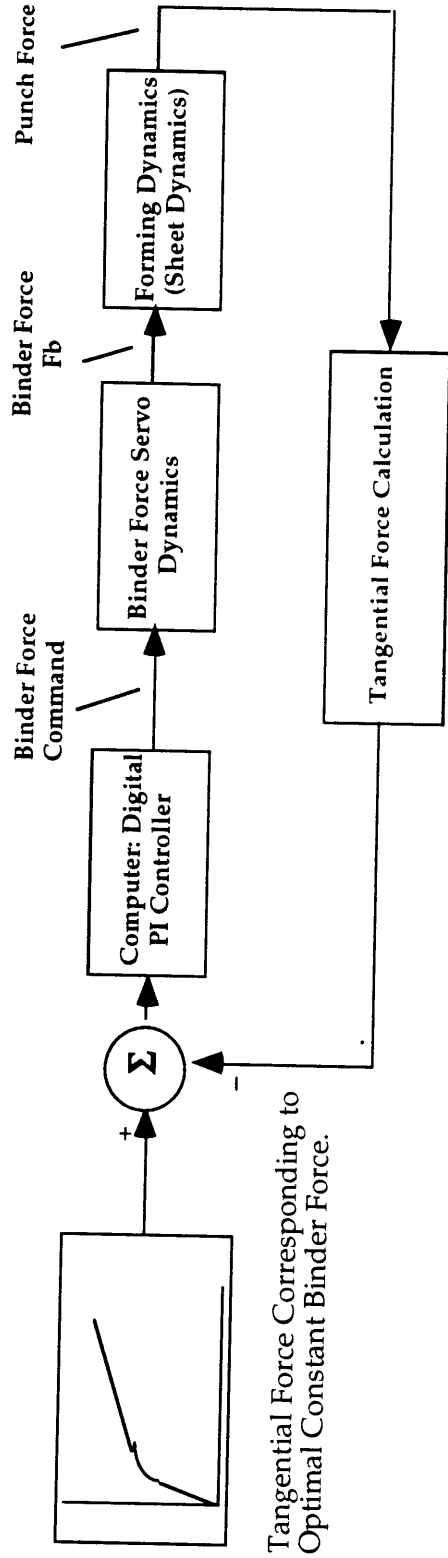


Figure 5.11 Closed Loop Block Diagram for a Tangential Force Reference

5.4.2 Results

The first set of experiments is conducted using the tangential force corresponding to the optimal CBF as a reference. In figure 5.12, the failure height is plotted versus the constant binder force for the open loop case and versus the initial binder force for the closed loop case. During the closed loop experiments, the cup is clamped at a given binder force far away from the CBF. The controller is turned on after a forming height of 0.3 inch since the tangential force data read is very noisy in this first stage of the experiment. As shown in figure 5.12, the cups produced fail at or near the optimum height regardless of the initial guess in the binder force. The performance of the control system is shown in figures 5.13 and 5.14 for experiments conducted at initial binder forces of 500, 2000 and 5000 lb (the optimal CBF being 1500 lb in this case). In figure 5.13, we show plots of the actual closed loop binder force trajectories versus the forming height. As expected, for the same amount of lubrication used in the open loop experiments (see Chapter 3), the binder forces converge to the optimal force (1500 lbs) in all three cases. Although the convergence is not very rapid, the failure height remains unaffected. In figure 5.14, the tangential forces for all three cases are plotted along with the reference tangential force (corresponding to the CBF). Again these forces all converge to the reference force. We note that in all three cases the tangential forces and the binder forces seem to be diverging away from the reference towards the end of the process. The reason for this behavior is understood when one looks at the tangential force reference in figure 5.14. This reference levels off towards the end of the process. As a result of this changing input, and since the control system is somewhat limited in its response time, the binder forces go through a second transient which explains the divergence from the optimal CBF.

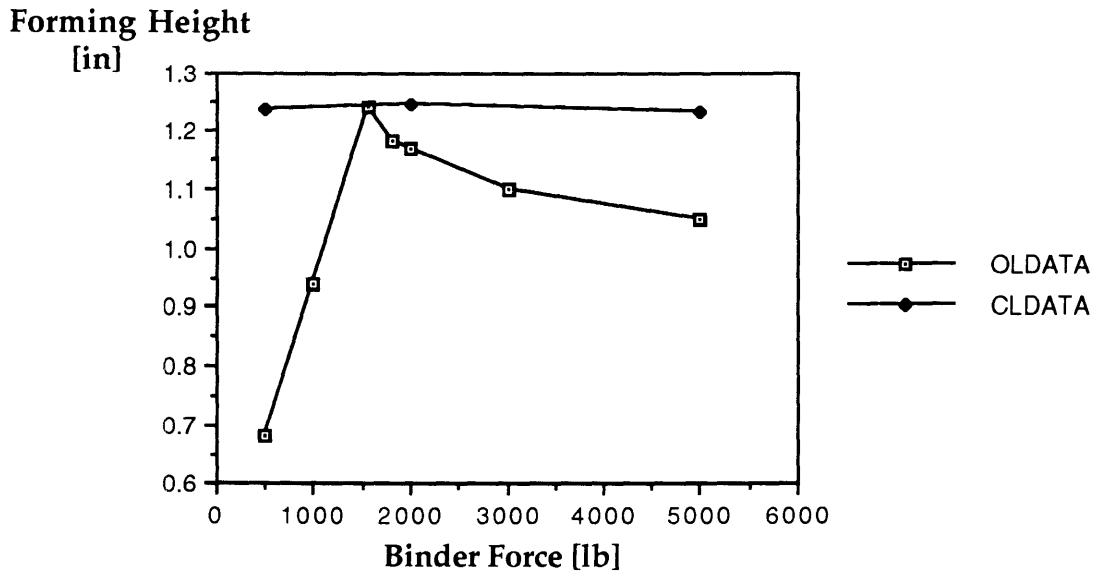


Figure 5.12 Forming Height Diagram For Al 2008-T4: Open Loop and Closed Loop Data.

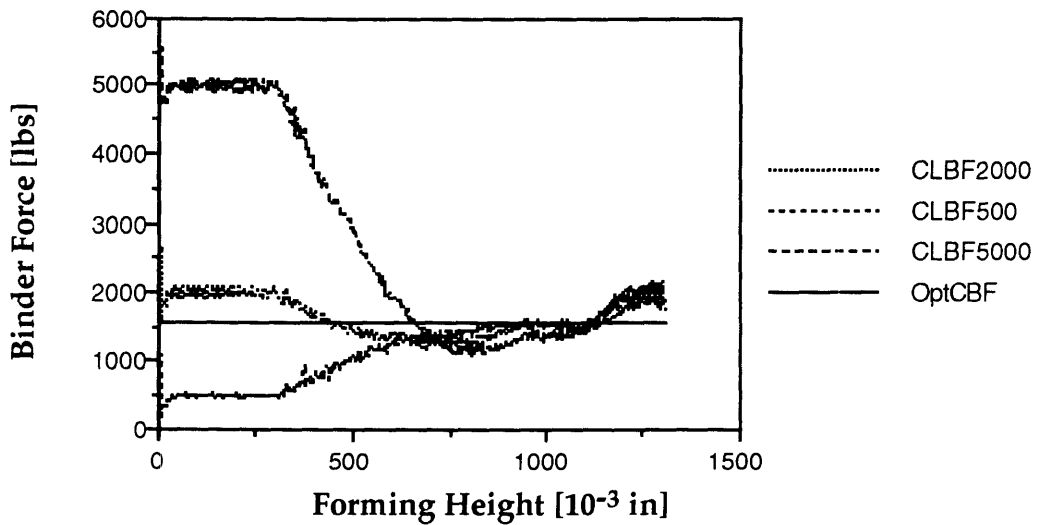


Figure 5.13 Closed Loop Binder Force Responses For Initial Binder Forces of 500, 2000 and 5000 lb.

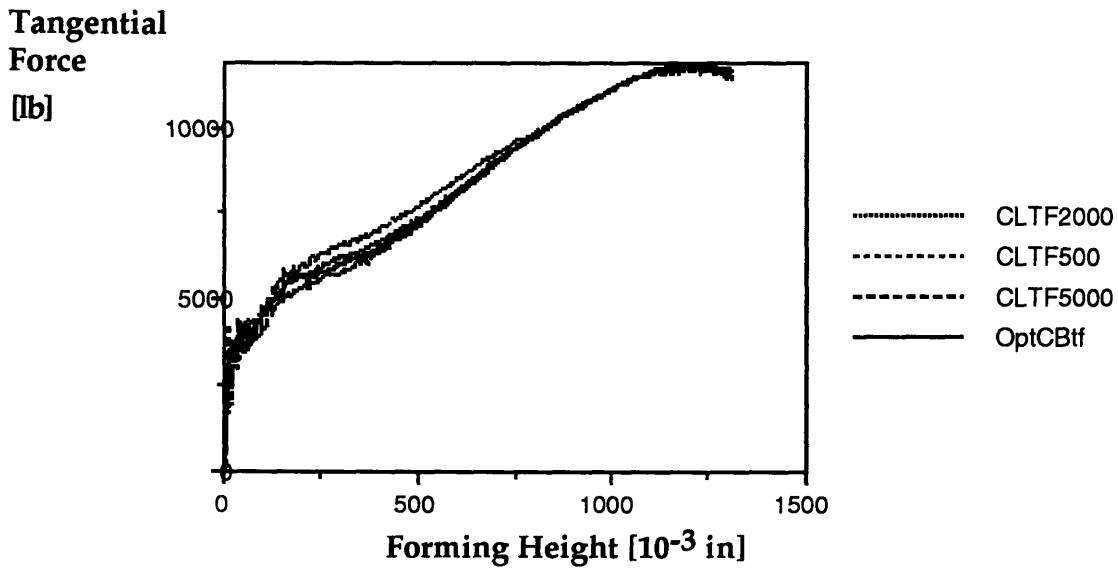


Figure 5.14 Closed Loop Tangential Force Responses For Initial Binder Forces of 500, 2000 and 5000 lb.

The second set of experiments corresponds to a tangential force reference obtained from the open loop variable binder force (VBF) experiment. In figure 5.15, we plot the binder force obtained from the closed loop experiment along with the VBF versus the forming height. Clearly, the plots show that the closed loop scheme does not track the desired open loop result for the same lubrication conditions. The proportional integral (PI) control algorithm is not converging. This poor result calls for a more sophisticated control algorithm. In order to devise one intelligently we will require to obtain a process model. This problem will be discussed extensively in the following section.

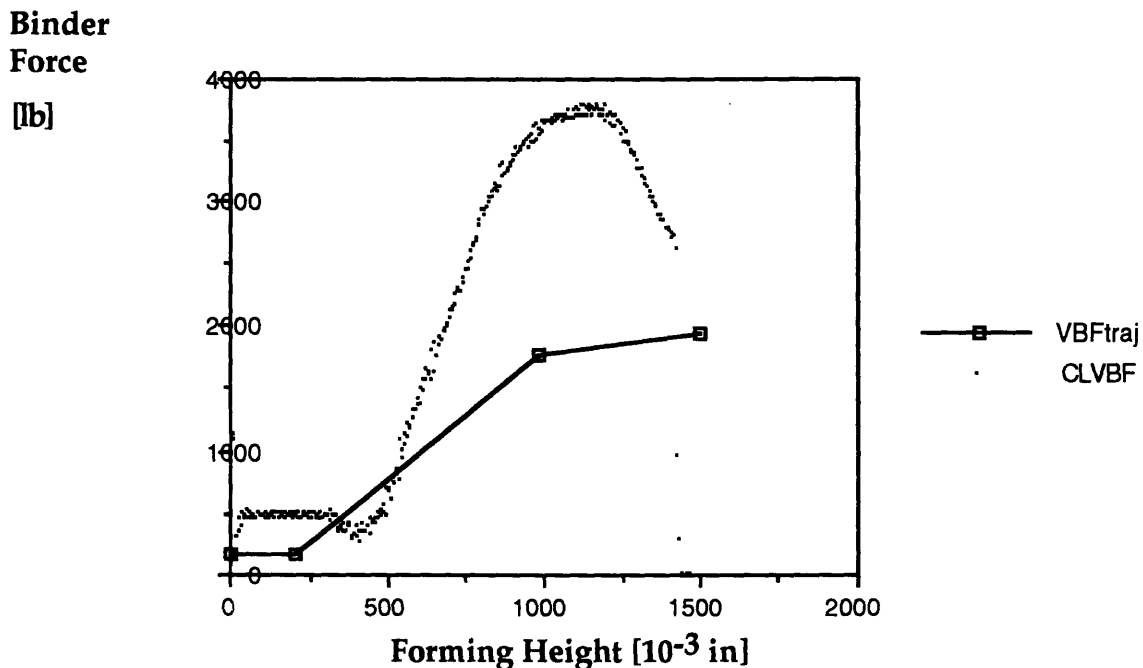


Figure 5.15 Closed Loop Binder Force Response to a Tangential Force Corresponding to the Optimal Variable Binder Force.

5.4.3 Discussion

As can be seen from the results of the first set of experiments, the closed loop experiments were successful in duplicating the open loop optimal constant binder force (CBF) forming conditions without any knowledge of what the optimal binder force should be. In this case, the results obtained show that the closed loop scheme is capable of converging to the desired forming conditions even when the initial conditions for the process are far off the desired conditions (e.g. experiment with initial binder force 5000 lb). In addition, since the reference input to the closed loop system is the tangential force in the part which is absolutely independent of the lubrication conditions in the flange area one can conduct these closed loop experiments without paying attention to the amount of lubrication used, while still consistently achieving optimal (CBF) results.

The second set of experiments was not successful however in tracking the open loop optimal variable binder force (VBF) experiments. As mentioned earlier, a process model is needed before proceeding any further with a control algorithm. Once a dynamic model is obtained, one can then devise a control algorithm either analytically (if an

analytical expression of the process is obtained) or simply by simulation if the model is too complicated to be described by an analytical expression.

Nevertheless, the importance of the closed loop experiments lies beyond the results already obtained. Looking at figure 5.14, the tangential force converges to the reference late in the process. Each of these tangential forces corresponds to a given strain path. Since the strain paths are different, the amount of springback on each of the parts obtained will be different, which will result in shape variation in the parts produced. In the future once a process model is obtained, the closed loop dynamics speeded up and the tangential force reference accurately tracked, the closed loop process will provide us with the ability to track any strain path given (since all tangential forces obtained will be very similar). As a result, the parts obtained will have the same amount of springback and consequently the same shape.

Chapter 6

Conclusion, Present Research and Suggestions For Future Work

6.1 Summary and Conclusion

During this research project, the conical cup forming process was studied for three aluminum alloys (Al 2008-T4, Al 5754- HO and Al 6111-T4). An optimal constant binder force which gave the deepest forming height was found and a forming height diagram was constructed for all three materials for the specific geometry and the specific lubrication conditions. For binder forces lower than the optimum, the cups failed prematurely due to wrinkling in the upper and/or the lower portions of the unsupported area. For binder forces higher than the optimum, the cups failed prematurely due to tearing near the punch nose.

Although all three materials failed at about the same optimal forming height (1.225 inch), and possessed the same final draw-in at the optimal forming height, the optimal binder force was different from one material to another. The optimal constant binder force for Al 2008-T4 was 1500 lb while the optimal force for Al 5754-HO was 900 lb and the optimal force for Al 6111-T4 was 1500 lb. This difference is due to the fact that the lubricant used (see chapter 4) provides different friction conditions between the binder and the flange for each of the materials for a given binder force.

In addition, we notice that the similarity obtained in forming heights between the aluminum alloys does not extend to the AKDQ steel experiments conducted by Fenn. In the case of the steel experiments the forming height obtained was 1.375 inch which is considerably deeper than the aluminum optimal forming height. This result leads us to conclude that the tearing limit for steel is higher than its aluminum counterpart. In addition, the wrinkling limit (i.e the critical wrinkling stress) was also higher; otherwise, one can just lower the binder force and form the cups on the wrinkling side of the forming height diagram.

Although the optimal constant binder force provided the deepest forming height for the process among all the constant force trajectories, it does not necessarily guarantee the best usage of material and further improvement of the cup failure height was still possible. Based on the idea that more material be permitted to draw-in during the beginning of the process in order to enable greater material usage and then, at a later stage increase the binder force gradually and steadily to prevent wrinkling from occurring due to the development of high hoop stresses, a variable binder force trajectory was constructed and

followed. The final failure height was 11% higher than the earlier forming height obtained from the optimal constant binder force.

Finally, real-time closed loop control of the process using a proportional and integral (PI) controller was tested in order to overcome disturbances in the boundary conditions such as variation in the amount of lubrication or variation in the initial binder force. The average tangential force trajectory calculated from the punch force obtained during the optimal constant binder force experiment was used as a reference trajectory in the closed loop scheme. The method successfully formed cups to heights comparable with that of the optimal open loop experiment regardless of the initial binder force used. The closed loop system was stable and the tangential force converged to the optimal reference tangential force. Unfortunately, the convergence of the closed loop scheme was not as fast as desired. As a result, given an initial binder force, one cannot subject all the cups to a unique strain path since the desired tangential force cannot be followed during the early stage of the forming process. Consequently, the amount of springback varies from one cup to another thereby causing a variation in the final shapes of the formed cups.

Eventhough the closed loop experiments were successful in tracking the tangential force corresponding to the open loop constant optimal binder force, this was not the case for the closed loop experiment corresponding to the open loop variable binder force. We are therefore unable to form deeper cups in a consistent disturbance free fashion.

The need to form deeper cups along with the need to control the springback of the successful cups formed, calls for a better control algorithm that will track the tangential force trajectory faster. In order to devise a high bandwidth algorithm, the process dynamics should be well understood. Therefore, a process model is needed!

6.2 Present On-Going Research: Cup Forming Process Model.

6.2.1 Method of Approach.

To properly model the dynamics of any system one may try to write the force equilibrium equations, the force-deformation relations and finally the geometric compatibility relations. In this case, since the process involves plastic deformation and because the stress strain relations are extremely messy it is virtually impossible to write down the force-deformation relations. In addition, it is also difficult to model the friction conditions under the binder and especially around the inner binder radius. In this case, the only option left is to identify the dynamics of the process from experimental results. Already, one can determine the binder force to tangential force steady state relation from the

constant binder force experiments. The transient behavior however is determined by subjecting the cup to increasing and decreasing step changes in the binder force at different stages in the process. Since the controller is activated at the forming height of 0.3 inch, the study of the dynamics will concentrate on the stages beyond this forming height.

6.2.2 Steady State Behavior

In figure 5.2, we show the tangential force responses to different constant binder force inputs. We notice that the slope of the tangential force increases with the increase in the binder force magnitude. Each of the tangential force curves can be approximated by an affine function, which is a fairly accurate assumption for forming heights greater than 300 mils. Mathematically, we can express this dependency of the tangential force on the binder force in the following manner

$$\frac{\partial F_t}{\partial h} = F(F_b) \quad (6.1)$$

Integrating with respect to h we obtain

$$F_t = F(F_b) \cdot h + G(F_b) \quad (6.2)$$

Fitting all these curves we have

$$F_t = F_o(F_b) \cdot (0.002 \cdot h + 1) \quad (6.3)$$

Where F_o is shown in figure 6.1.

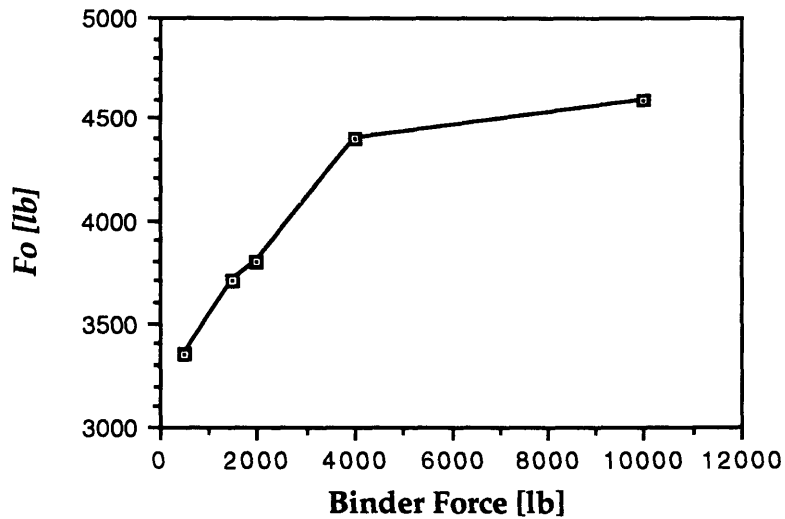


Figure 6.1 Factor Relating The Tangential Force to The Binder Force in Steady State.

Notice in the range where the binder force is lower than 4000 lb, the steady state relation between the tangential force and the binder force is linear and the steady state relation becomes

$$\frac{F_t}{F_b} = 0.3 \cdot (0.002 \cdot h + 1) \quad (6.4)$$

Physically, this relation is expected. A constant binder force should cause a steady increase in the tangential force since, as the forming progresses the forming angle Θ (shown in figure 4.2) increases, which causes an increase in the frictional forces between the binder radius and the sheet thereby causing an increase in the tangential force.

6.2.3 Transient Behavior

The transient behavior is captured by varying the binder force input during the process. In figure 6.2, both the binder force input and the tangential force response are plotted versus the forming height. The binder force input is a square wave ranging between 1550 and 10000 lb. In the case where the binder force is increasing (stepwise), the tangential force goes through a transient, where it increases at a sharp rate then settles at a

rate steeper than the original one. A quick look at figure 6.3 shows the draw-in to be constant during the transient. The obvious conclusion in this case is: during the transient the cup is undergoing pure stretching with no material flowing in the unsupported area. In the case of the decreasing (step) binder force however, the tangential force exhibits no transient behavior but instead jumps to a lower magnitude then settles at a rate lower than the previous one. This no transient behavior is due to the elastic retraction of the material due to the sudden drop in the stretching (or binder) force. Another phenomenon to observe: the tangential force becomes evermore sensitive to binder force step changes as the forming process progresses.

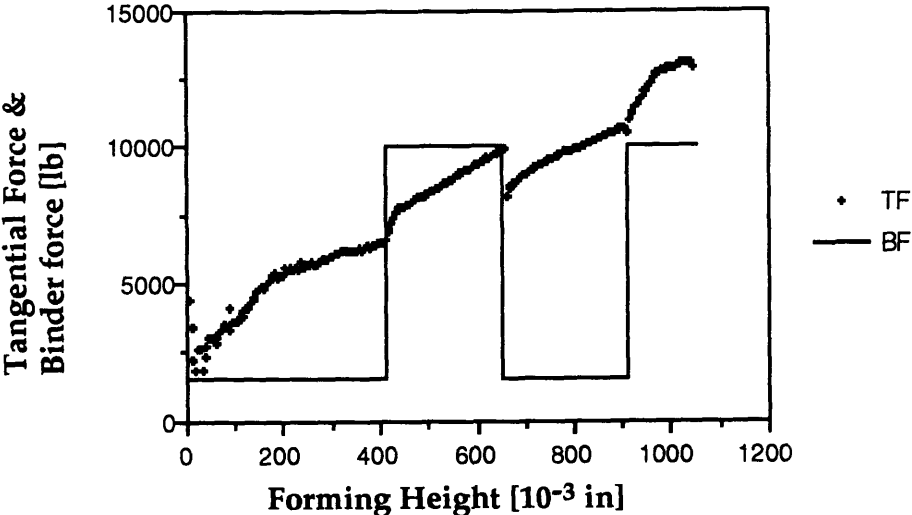


Figure 6.2 Tangential Force Response to a Binder Force Square Wave between 1550 and 10000 lb.

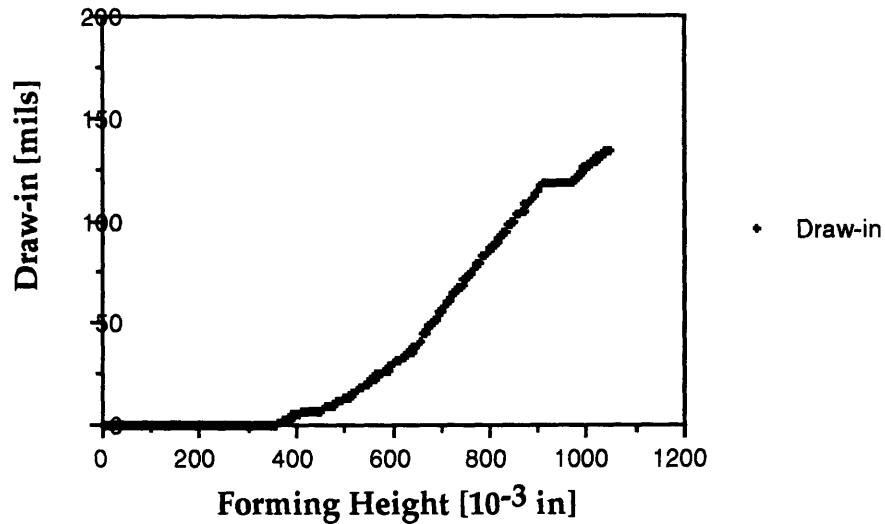


Figure 6.3 Draw-in Response to a Binder Force Square Wave between 1550 and 10000 lb.

Clearly, The dynamics relating the binder force to the tangential force depend on the direction of change of the binder force. Each of these dynamics need to be analyzed separately.

6.2.4 Dynamics Corresponding to a Decreasing Binder Force

The results obtained from the steady state behavior show that the steady state relation between the binder force and the tangential force is linear given that the binder force is lower than 4000 lb. Moreover, this relation may suggest that the system is equivalent to a pure integrator system. This is not true however. The step decrease in the tangential force due to a step decrease in the binder force suggests that the system exhibits some kind of proportional action. Combining both transient and steady state behavior, we obtain the following transfer function

$$\frac{F_t}{F_b} = K_p + \frac{K_i}{s} \quad (6.5)$$

where K_p and K_i are the proportional and integral gains respectively, s the Laplace variable with respect to the forming height, and

$$K_i = 0.0006.$$

(6.6)

Since K_p varies during the process, we compute it experimentally for step changes in the binder force ranging between 1500 and 4000 lb. Figure 6.4 shows the values of the proportional gain at different stages of the process.

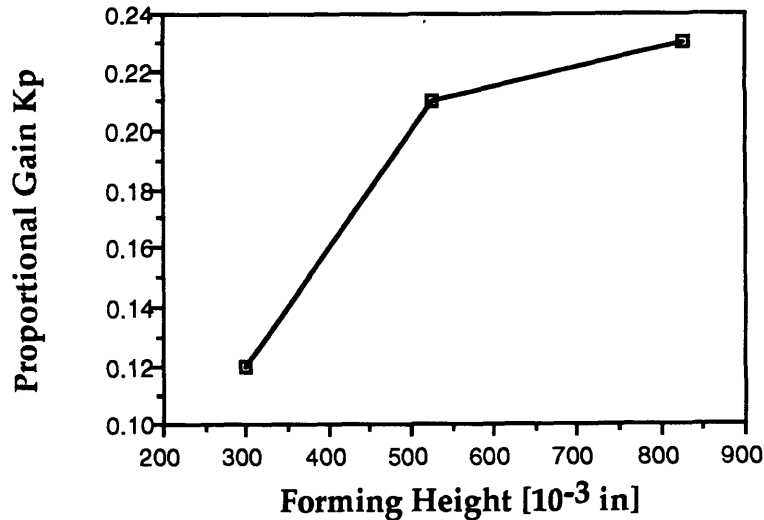


Figure 6.4 Proportional Factor in Transfer Function Relating The Tangential Force to The Binder Force.

6.2.5 Closed Loop Simulation Results

Having made an initial attempt at modeling the process in the case of a constant or decreasing binder force input, the focus is now to model the case where the binder force is increasing. Having already established that in this case, during the transient, the sheet is undergoing pure stretching, the rate of increase of the tangential force is maximum (10 lb/mil) and constant (See figure 6.5). Using this addition to the previous model as an initial guess of the increasing binder force dynamics we obtain transiential dynamics in figure 6.5, similar to the experimentally observed dynamics in figure 6.2. In order to test the constructed model, the closed loop experiments depicted in chapter 5 for the CBF experiments are simulated for the same initial conditions (500, 2000 and 5000 lb). The simulation results along with the experimental results are shown in figures 6.6, 6.7 and 6.8.

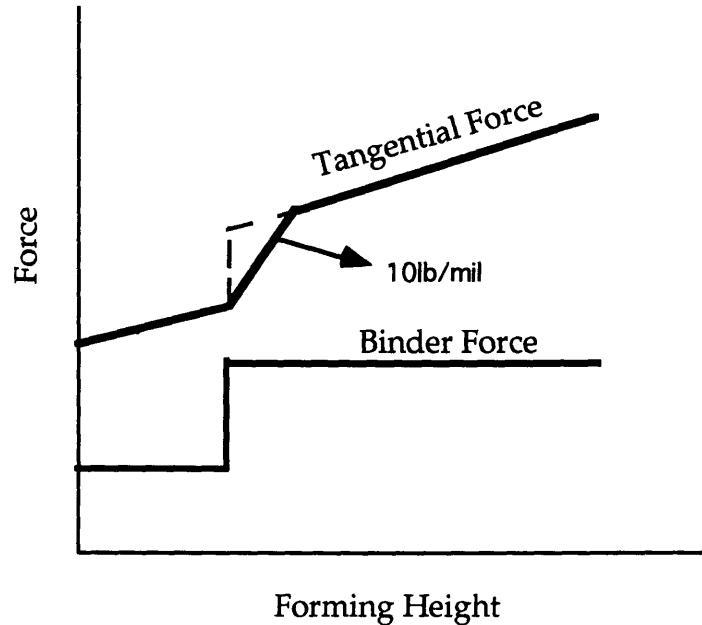


Figure 6.5 Rate Limiter Addition to the Original PI Model.

6.2.6 Discussion and Suggestions For Future Research.

The simulation results obtained in figures 6.6, 6.7 and 6.8, show that the simulated binder force response follows the experimental binder force accurately in the cases where the binder force is decreasing. However, this is not the case when the binder force is increasing. This is why the simulated results in figures 6.6 and 6.7 follow the experimental results very closely up to the stage where the binder force begins increasing. This is also why the simulation shown in figure 6.8 does not agree with the experiment at all. We therefore conclude that the model obtained for the case where the binder force is decreasing is fairly accurate, while the model obtained for the case where the binder force is increasing clearly needs improvement.

In the future, the logical next step would be to analyze the dynamics for the increasing binder force case in order to improve the existing model. Once completed, the model can be used to design a controller to improve the closed loop tangential force tracking response for the CBF case. It can also be used to design a control algorithm to accurately track the tangential force reference obtained from the VBF experiment.

Once tracking is obtained with adequate speed, deeper aluminum cups can be formed with consistent shape. Having achieved that, the technical problems associated with

aluminum forming would be solved. At that point, the issues associated with cost should be addressed.

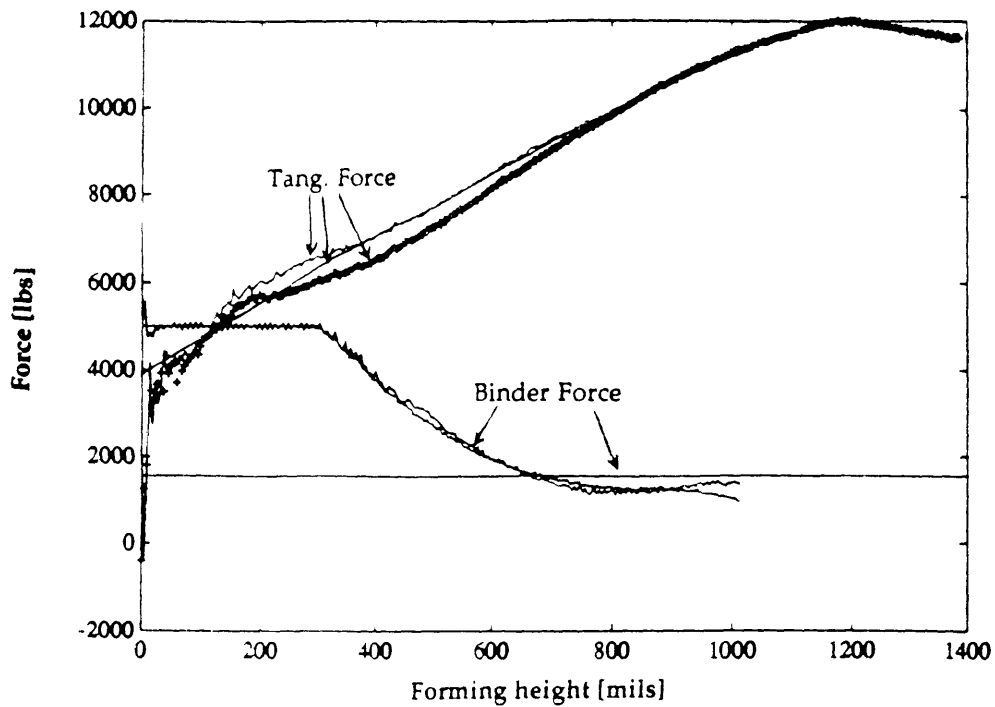


Figure 6.6 Closed Loop Simulated and Experimental Binder Force and Tangential Force Responses for an Initial Binder Force of 5000 lb.

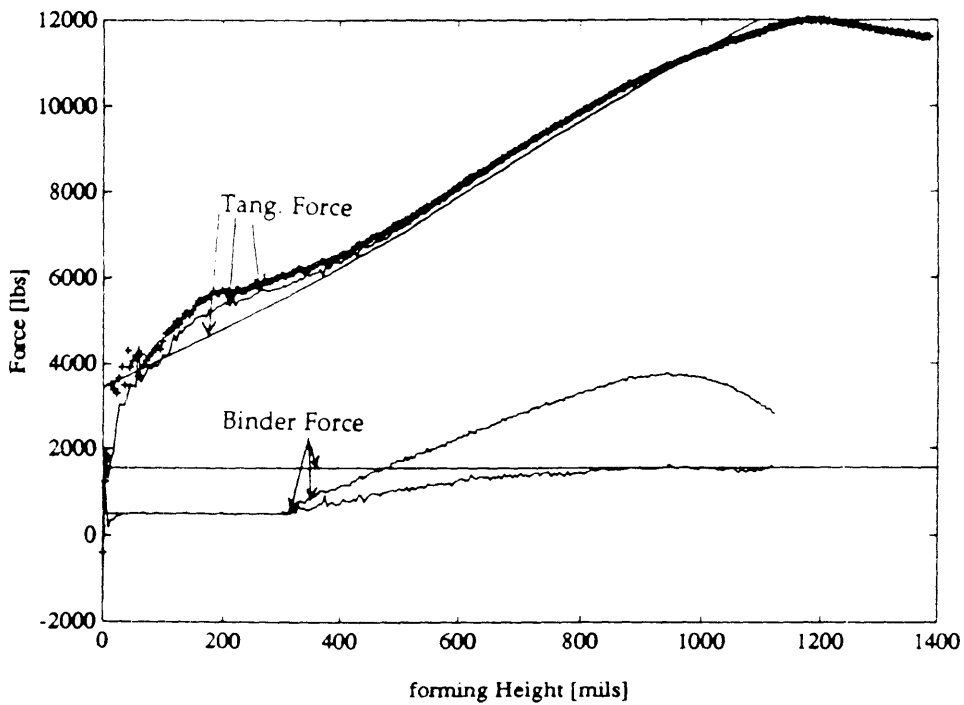


Figure 6.7 Closed Loop Simulated and Experimental Binder Force and Tangential Force Responses for an Initial Binder Force of 2000 lb.

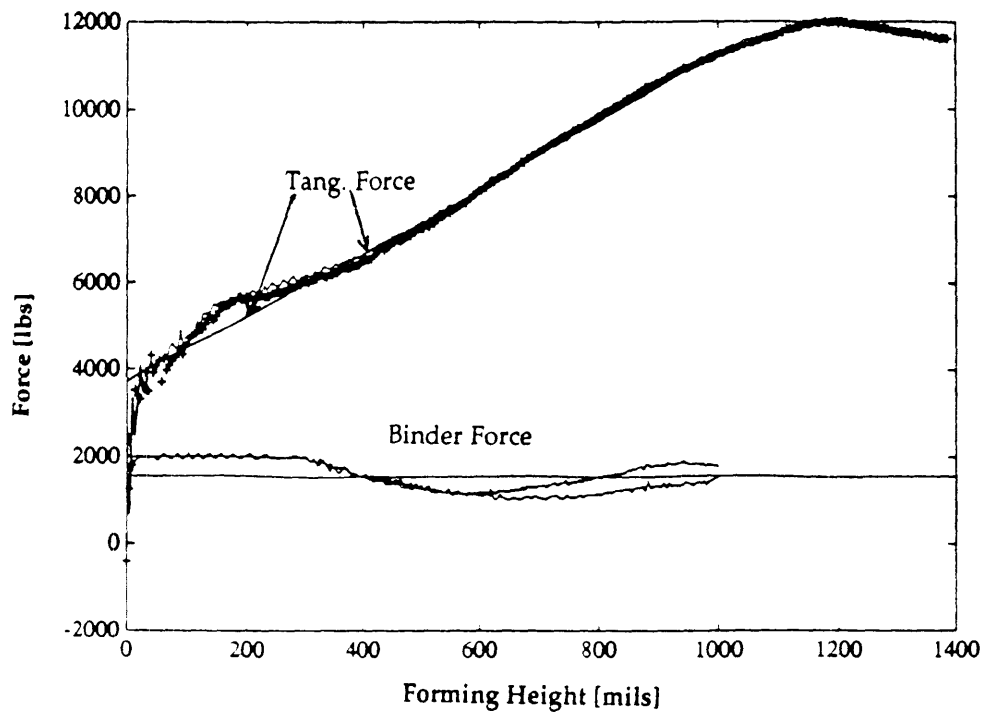


Figure 6.8 Closed Loop Simulated and Experimental Binder Force and Tangential Force Responses for an Initial Binder Force of 500 lb.

Bibliography

- [1] Beckwith, Thomas G., Buck, N. Lewis and Marangoni, Roy D. (1989) “Mechanical Measurements”, Third Edition, Addison-Wesley Publishing Company, Inc., Philippines.
- [2] Ogata, Katsuhiko (1990) “Modern Control Engineering”, Second Edition, Prentice Hall Inc., Englewood Cliffs, New Jersey 07632
- [3] Hosford, William F. and Caddell, Robert M. (1983), “Metal Forming: Mechanics and Metallurgy”, Prentice-Hall, Englewood Cliffs, N.J.
- [4] Kalpakjian, Serope (1984), “Manufacturing Processes for Engineering Materials”, Addison-Wesley Publishing, Reading, Massachusetts.
- [5] Data Translation (1984) User Manual for DT2801 Series, Third Edition.
- [6] Data Translation (1990) User Manual for DT2811 Series, Fifth Edition.
- [7] Fenn, R.C., (1989) “Closed Loop Control of Sheet Metal Stability During Stamping”, Ph.D. Thesis, Massachusetts Institute of Technology, Dept. Mechanical Engineering.
- [8] Lee, C. G. Y., (1986) “Closed Loop Control of Sheet Metal Stability During Forming”, S.M. Thesis, Massachusetts Institute of Technology, Dept. Mechanical Engineering.
- [9] Fenn, R., and D.E. Hardt (1990) “Real-Time Sheet Forming Stability Control”, Proc. International Deep Draw Research Group, June, Stockholm.
- [10] Hirose Y., Hishida, Furubayashi, T., Oshima, M., and S. Ujihara (1990) “Part I: Techniques for Controlling Wrinkles by Controlling the Blank Holding Force”, Proc. 4th Symposium of the Japanese Society for the Technology of Plasticity.
- [11] Hirose Y., Hishida, Furubayashi, T., Oshima, M., and S. Ujihara (1990) “Part II: Application of BHF-Controlled Forming Techniques”, Proc. 4th Symposium of the Japanese Society for the Technology of Plasticity.

[12] Sim, H.B. (1990) "Numerical Simulations of Stability Control in Sheet Metal Forming", S.M. Thesis, Massachusetts Institute of Technology, Dept. Mechanical Engineering.

[13] Sim H.B., and M.C. Boyce (1992) "Finite Element Analysis of Real-Time Stability Control in Sheet Forming Processes", *ASME Journal of Engineering Materials and Technology*, 114.

[14] Jalkh, P., Cao, J., Hardt, D., and Boyce, M.C. (1992) "Optimal Forming of Aluminum 2008-T4 Conical Cups Using Force Trajectory Control",